Reviewed Preprint
v1 • November 21, 2025
Not revised

Reviewed Preprint
v2 • June 19, 2026
Revised by authors

For correspondence:
oxana.eschenko@tuebingen.mpg.de

§ Present address: Department of Brain-Body Cybernetics, Max Planck Institute for Biological Cybernetics, Tübingen, Germany

Competing interests: No competing interests declared

Funding: See page 21

Reviewing editor: Adrien Peyrache, McGill University, Canada

Differential locus coeruleus–hippocampus interactions during offline states

Mingyu Yang, Oxana Eschenko[§]

Department of Physiology of Cognitive Processes, Max-Planck Institute for Biological Cybernetics, Tübingen, Germany

eLife Assessment

This **important** study provides new insights into the neuronal dynamics of the locus coeruleus in relation to hippocampal sharp-wave ripples. Using high-temporal-resolution, multi-site electrophysiological recordings in rats, the authors present **convincing** evidence that ripples and locus coeruleus activity are inversely correlated to levels of arousal and noradrenaline tone is modulated by hippocampo-cortical coupling. Overall, the work will be of interest to neuroscientists studying large-scale brain coordination and memory processes.

https://doi.org/10.7554/eLife.109159.2.sa4

Abstract

Patterns of locus coeruleus (LC) activity and norepinephrine (NE) release during non-rapid-eye-movement (NREM) sleep suggest a critical role for the LC–NE system in offline modulation of forebrain circuits. NE transmission promotes synaptic plasticity and is required for memory consolidation, but the field has only begun to uncover how LC activity contributes to coordinated forebrain network dynamics. Hippocampal ripples, a hallmark of memory replay, are temporally coupled with thalamocortical oscillations; however, the circuit mechanisms underlying systems-level consolidation across larger brain networks remain incompletely understood. Here, using multi-site electrophysiology, we examined LC firing in relation to hippocampal ripples in freely behaving rats. LC activity and ripple occurrence were state-dependent and inversely related: heightened arousal was associated with increased LC firing and reduced ripple rates. At finer timescales, LC spiking decreased ~1–2 seconds before ripple onset, with the strongest modulation during awake ripples but minimal change during ripple–spindle coupling. These findings reveal state-dependent dynamics of LC-hippocampal interactions, positioning the LC as a key component of a cortical–subcortical network supporting systems-level memory consolidation.

Introduction

Norepinephrine (NE) modulation of the forebrain circuits supporting cognition has long been considered to play a role during vigilant states (Sara, 2009; Sara and Bouret, 2012), whereas its impact during low arousal (or 'offline') states, including sleep, has received less attention. The pioneering discovery of greatly reduced firing of the locus coeruleus (LC) neurons during sleep (Aston-Jones and Bloom, 1981), for decades, directed research focus toward the role of LC, as a part of the ascending arousal system, for 'online' information processing. At the same time, pharmacological studies in both animals (Sara et al., 1999; Roullet and Sara, 1998; Clayton and Williams, 2000; Galeotti et al., 2004; Gazarini et al., 2013) and humans (Groch et al., 2011; Gais et al., 2011; Kuffel et al., 2014; Cahill et al., 1994) have demonstrated the importance of post-learning NE transmission for memory consolidation. The results of pharmacology studies

were consistent with a well-established facilitatory role of NE for synaptic plasticity, which also takes place offline (Straube and Frey, 2003; Gelinas and Nguyen, 2005; Harley, 2007; Hansen and Manahan-Vaughan, 2015; Hagena et al., 2016; Palacios-Filardo and Mellor, 2019).

During offline states such as awake immobility and non-rapid eye movement (NREM) sleep, hippocampal activity is marked by transient episodes of synchronized firing, detected in CA1 local field potentials (LFPs) as high-frequency ~150 Hz oscillations known as ripples Buzsaki (1996). Hippocampal ripples, a hallmark of memory replay, are temporally coupled with thalamocortical sleep spindles (10–16 Hz) and cortical slow (~1Hz) oscillations, which together represent key components of the mechanism underlying systems-level memory consolidation (Klinzing et al., 2019). In recent years, it became evident that ripples reflect not only a coordinated local activity within the hippocampus but also indicate the emergence of large-scale functional networks (Logothetis et al., 2012; Nitzan et al., 2022). The ripple-associated cross-regional communication may occur through a coordinated up/down-regulation of neural activity across cortical and subcortical structures, including neuromodulatory centers (Skelin et al., 2018; Maingret et al., 2016; Brodt et al., 2023). Several studies have demonstrated temporally coordinated cross-regional neuronal activity around ripples, involving the amygdala (Girardeau et al., 2017), the ventral tegmental area (Gomperts et al., 2015), the median raphe (Wang et al., 2015), and the thalamus (Logothetis, 2015; Yang et al., 2019; Varela et al., 2001).

While some indirect evidence suggests a link (Logothetis et al., 2012), the relationship between LC neuron spiking and hippocampal ripples has not been directly characterized. For example, a study in the murine slice showed that increasing NE concentration increased ripple incidence and their amplitudes (Ul Haq et al., 2012). Consistently, in behaving rats, we showed that pharmacological suppression of NE transmission decreased the occurrence of ripples and impaired spatial memory consolidation (Duran et al., 2023). Finally, experimentally induced LC activation affected the temporal pattern of ripple occurrence (Novitskaya et al., 2016; Swift et al., 2018). Earlier studies have shown close temporal relations between LC and sleep spindles (Aston-Jones and Bloom, 1981; Swift et al., 2018; Osorio-Forero et al., 2021; Kjaerby et al., 2022). In our previous work, we have shown that firing of a subpopulation of LC neurons was temporally coordinated with slow oscillations (Eschenko et al., 2012; Totah et al., 2018), which in turn orchestrate spindle and ripple activity (Molle et al., 2006).

In the present study, we characterized the ripple-associated LC firing patterns in freely behaving rats. We report that LC activity was anticorrelated with the ripple rate at both large and fine temporal scales. Our results also provide evidence for a state-dependent engagement of the LC in offline memory processing and hippocampal-cortical communication.

Results

We analyzed a total of 20 recording sessions (n = 7 rats, 2 to 8 sessions per rat with an average duration of 6458.48 ± 190.43 sec), including two datasets (n = 1 rat) that contributed to our previous publication (Eschenko et al., 2012). All datasets contained simultaneously recorded extracellular spikes of putative LC-NE neurons, local field potentials (LFPs) from the CA1 subfield of the dorsal hippocampus (HPC), and frontal EEG (Figure 1). The recordings were performed in freely behaving adult male rats placed in a small chamber (30 × 30 × 40 cm) in dim light during the dark phase of the animal's circadian rhythm. Electrode positioning was fine-tuned using movable microdrives to ensure optimal detection of hippocampal ripples and LC spikes. The recordings from putative LC-NE neurons were verified using multiple electrophysiological criteria (see Methods for details), and the recording sites were additionally confirmed by histological examination (Figure 1B). The average firing rate of LC single units was 1.70 ± 0.21 Hz during wakefulness, 0.51 ± 0.07 Hz during NREM sleep, and 0.014 ± 0.01 Hz during REM sleep, differing significantly across arousal states (one-way ANOVA: $F(2,38) = 39.8$, $p < 0.0001$; Supplementary Figure 1). This firing pattern is characteristic of LC-NE neurons and is consistent with existing literature (Aston-Jones and Bloom, 1981; Eschenko et al., 2012; Eschenko and Sara, 2008; Hayat et al., 2020; Takahashi et al., 2010).

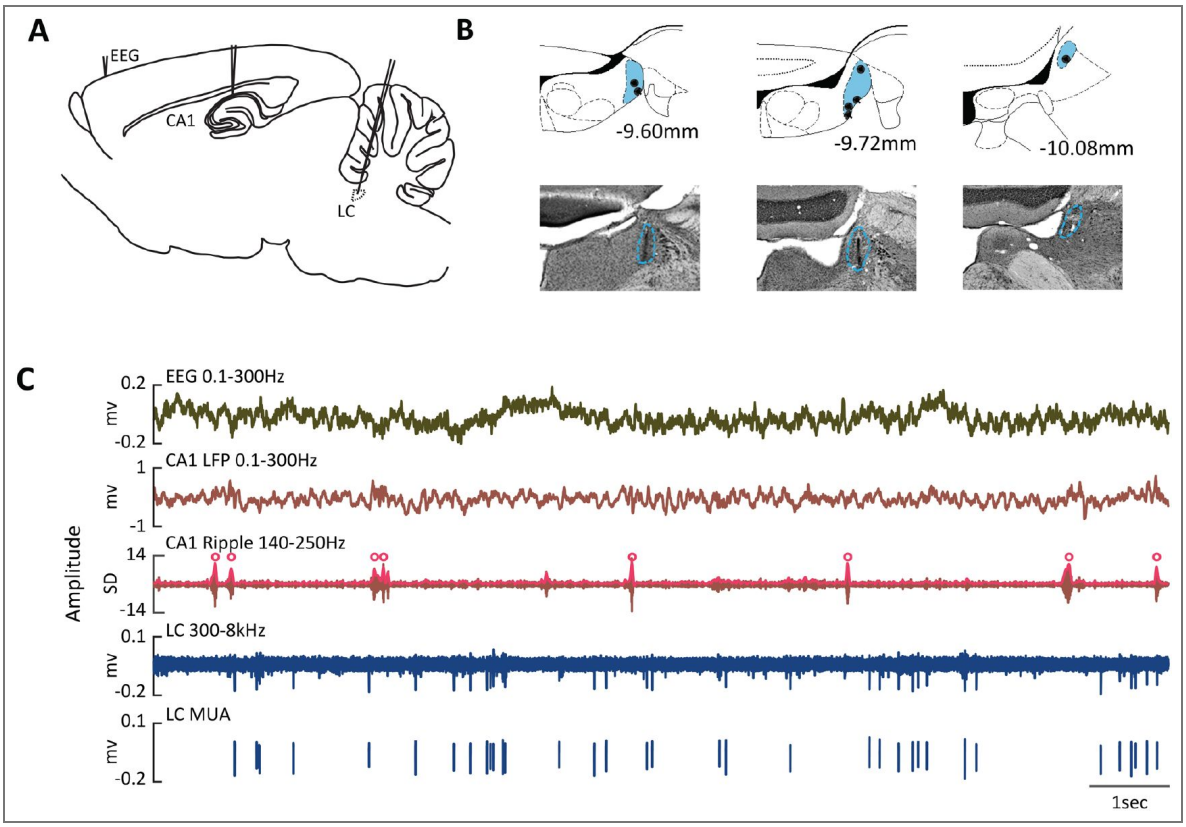

Figure 1. Multi-site extracellular recordings in freely behaving rats.

(A) Schematic of chronically implanted electrodes for recording the frontal EEG, local field potentials (LFPs) in the dorsal hippocampus (CA1), and neuron spiking in the locus coeruleus (LC). **(B)** Histological verification and reconstruction of electrode placements (black dots) within the LC (blue area). Numbers indicate anterior–posterior coordinates relative to bregma (Paxinos and Watson, 2005). **(C)** Representative traces of simultaneously recorded EEG, hippocampal LFPs, and LC neuron spikes during quiet awake. Red dots indicate hippocampal ripples.

LC-NE neuron spiking is suppressed around hippocampal ripples

We first characterized the temporal relationships between the LC neuron spiking and ripple occurrence. Ripples were detected from a power envelope of a band-passed (140 - 250 Hz), smoothed (at 25 Hz), and z-score normalized CA1 LFPs (Figure 1C). The average ripple rate (18.2 ± 1.5 ripples/min) was with a ripple amplitude of 10.3 ± 0.3 standard deviation (SD). There was a robust CA1 LFP power increase in the ripple band (140 - 250 Hz) around peaks of detected ripples (Figure 2A) and a transient power increase in the EEG delta (1 - 4 Hz) and spindle (12 - 16 Hz) bands (Figure 2B) immediately after the ripple onset, most likely reflecting the well-known temporal coupling of ripples with slow waves and sleep spindles (Molle et al., 2006).

The LC multiunit activity (LC-MUA) was extracted by thresholding a high-pass filtered (300 Hz – 8 kHz) extracellular signal recorded from the LC (Figure 1C). To directly compare the ripple-related LC activity dynamics, for each recording session, we computed the LC-MUA firing rate in a [-6, 6] sec window centered on the ripple onset, z-scored, and averaged across all detected ripples. This analysis revealed a prolonged and consistent suppression of LC activity both before and after ripple onset, with peak suppression < -2 SDs in all sessions (Figure 2C). In six out of twenty recording sessions, we could reliably isolate spikes from a total of 15 single units (n = 4 rats). The peri-ripple (± 6 s) firing suppression of LC single-unit activity (LC-SUA) exceeding the significance threshold of 2 SDs was observed in 13 of 15 cases (Figure 2D).

To quantify the peri-ripple LC activity change, we extracted the modulation onset time, duration, and magnitude, as illustrated in Figure 2D. The modulation magnitude (through on the perievent histogram) was greater for LC-MUA (-6.83 ± 0.84 SDs) compared to LC-SUA (-4.01 ± 0.65 SDs). Despite the difference in the modulation magnitude (Kolmogorov–Smirnov test, p = 0.019), the temporal profile of both LC-MUA and LC-SUA around ripples was remarkably similar (Figure 2D). No significant differences were found in the onset of spiking suppression (MUA: -4.08 ± 0.71 sec vs. SUA: -2.90 ± 0.50 sec, p = 0.138), duration (MUA: 8.28 ± 1.37 sec vs. SUA: 5.16 ± 0.92 sec, p = 0.069), or peak time (MUA: -0.29 ± 0.04 sec vs. SUA: -0.35 ± 0.04 sec, p = 0.561). Together, these findings indicated that the majority of LC-NE neurons showed a stereotypic activity pattern around hippocampal ripples. Therefore, we used the LC-MUA datasets for subsequent analyses.

LC firing and ripple occurrence are state-dependent and inversely related

The LC activity around rippled was modulated at multiple temporal scales. In the previous section, we described a relatively sharp drop in the LC firing rate ~ 2 s before the ripple onset. To capture LC dynamics at longer temporal scales, we tested a range of time windows and found that a 12- s peri-event interval adequately represents LC activity dynamics. When computing peri-ripple LC firing over a [–12, 12] sec time window, we observed a decrease in LC activity beginning as early as ~10 s before the ripple onset (Supplementary Figure 2). We hypothesized that slower LC dynamics might be related to fluctuations of the global brain state. Indeed, transient spectral changes in the EEG coincided with the occurrence of hippocampal ripples (Figure 2B).

We thus examined the temporal relationships between the ripple and LC activity and ongoing cortical state. To this end, we computed the ripple and LC-MUA rates within 4-s windows and quantified the corresponding cortical state using a synchronization index (SI), calculated as a power ratio (1–4 Hz/30–90 Hz) of the frontal EEG. Figure 3A illustrates that a higher SI corresponded to a lower arousal state; this brain state was associated with more synchronized cortical population activity, a higher ripple rate, and reduced LC neuron firing. Across all sessions, SI values were negatively correlated with LC-MUA (Pearson correlation, r = –0.71 to –0.25, p < 0.01, the highest p = 0.0095; Figure 3B, upper panel) and positively correlated with the ripple rate (r = 0.10 to 0.50, p < 0.01, the highest p = 0.008). As shown in Figure 3B, LC activity was negatively correlated with both the SI and ripple rate (r = –0.38 to –0.11, p < 0.01, with the highest p = 0.0074, n = 20; Figure 3B, lower panel). Together, these results demonstrate that LC activity, cortical state, and ripple occurrence are strongly interrelated, suggesting that the slow (multi-second) dynamics of peri-ripple LC modulation may, in part, reflect underlying brain-state fluctuations.

Figure 2. **LC-NE neuron spiking is suppressed around hippocampal ripples.**

(A, B) Representative peri-ripple spectrograms of CA1 LFPs **(A)** and frontal EEG **(B). (C)** Normalized peri-ripple LC multi-unit activity. Each row represents an individual dataset, with the overlaid trace showing the average across sessions. **(D)** Comparison of peri-ripple LC multi- and single-unit firing. Normalized firing rates were averaged and smoothed with a 1 Hz low-pass filter. The dashed line marks the 1 SD threshold used to define the onset and offset of ripple-associated LC modulation. The modulation magnitude was extracted as a through on the peri-event histogram.

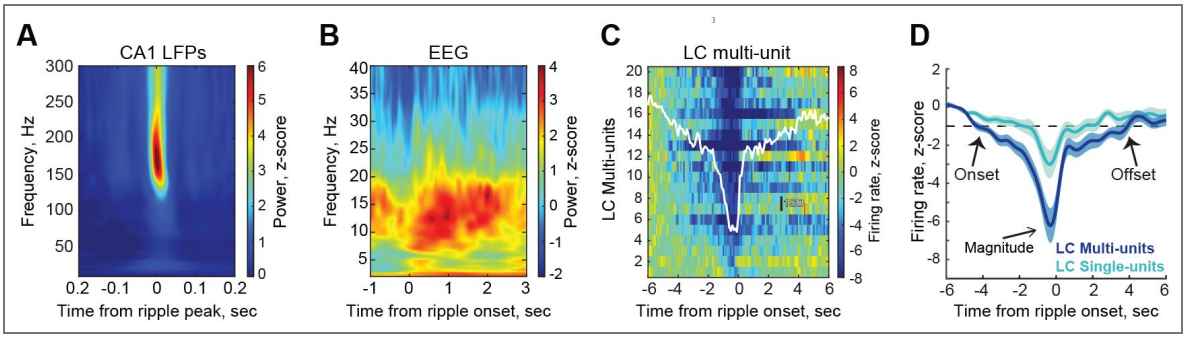

Figure 3. **The relationship between LC activity and hippocampal ripples at multiple temporal scales.**

(A) Representative traces showing the relationship among cortical state, LC neuron spiking, and ripple rate. Cortical state was quantified by the Synchronization Index (SI), calculated as the ratio of the EEG delta (1–4 Hz) to gamma (30–90 Hz) power. Higher SI values, reflecting a more synchronized cortical state, were associated with lower LC activity and higher ripple rates. **(B)** An example of correlation between LC-MUA and SI (upper panel) and between LC-MUA and ripple rate (lower panel) obtained from the same recording session. **(C)** Mean CA1 LFPs ripple-band (140–250 Hz) power aligned to the ripple onset (purple) or shuffled events (pink). **(D)** Average Synchronization Index (SI) around ripples and shuffled events. The cortical state preceding shuffled events and ripples was comparable, as confirmed by the absence of significant differences in SI (Wilcoxon signed-rank test; shuffled: Z = -0.20, p = 0.84; ripples: Z = 0.14, p = 0.88). Cortical synchrony increased following both events (shuffled: Z = -3.50, p = 0.00044; ripples: Z = -3.66, p = 0.00026). Similar cortical state dynamics surrounding shuffled events and ripples indicate that the surrogate events adequately capture the cortical state associated with ripple occurrence. **(E)** Normalized peri-ripple LC-MUA for individual sessions. **(F)** Session-averaged peri-ripple LC-MUA. The shaded area denotes the [-1, 0 sec] time window used for the Modulation Index (MI) calculation.

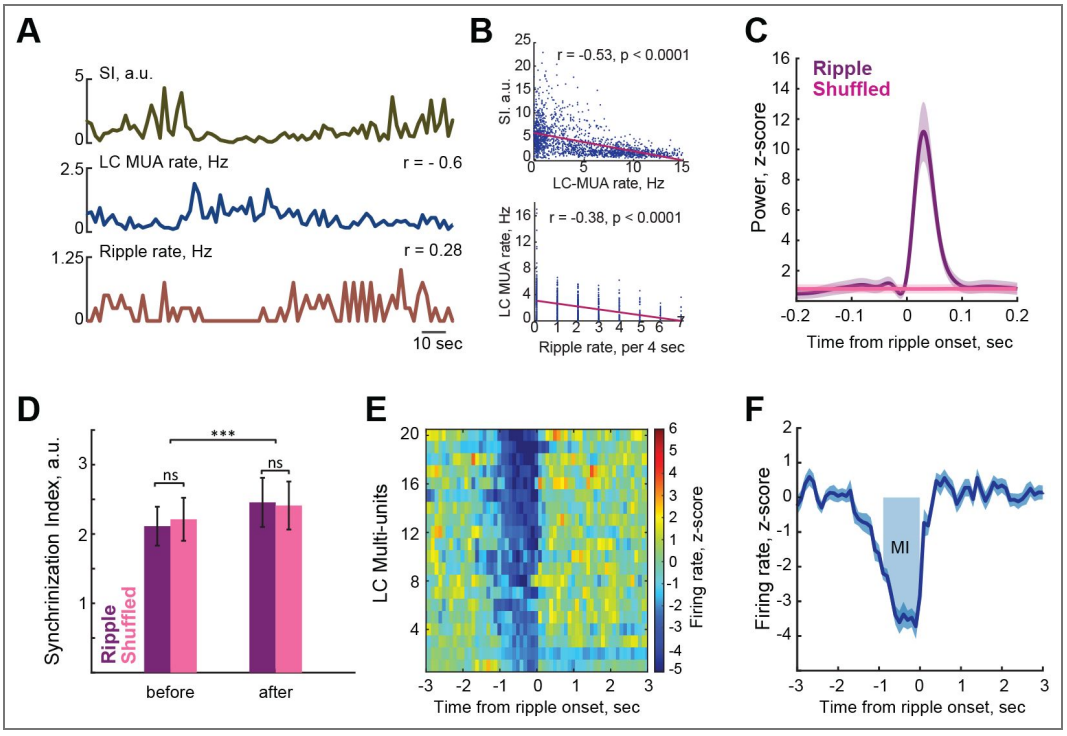

To account for the potential influence of global brain state on peri-ripple LC activity, we generated surrogate events for each session by jittering the timestamps of detected ripples (see Methods). We first verified that hippocampal CA1 LFPs (140–250 Hz) triggered on these surrogate events lacked the ripple-specific frequency component (Figure 3C) and that the shuffled events adequately captured the cortical state dynamics associated with ripples (Figure 3D). Thus, LC activity aligned to surrogate events captured its state-dependent dynamics (Supplementary Figure 2). To isolate peri-ripple LC modulation from state-dependent fluctuations of the LC activity, we subtracted the LC-MUA around shuffled events from the peri-ripple LC-MUA for each session. The resulting traces provided a state-corrected estimate of ripple-associated LC activity, largely free from confounding effects of cortical state transitions. This analysis revealed a consistent suppression of LC activity at a finer temporal scale (1–2 s), although the temporal profile and magnitude of modulation varied across sessions (Figure 3E).

To quantify the degree of peri-ripple LC activity modulation, we extracted the onset time and the duration as illustrated in Figure 2D. In addition, we calculated the modulation index (MI) as the area under the curve of the session-averaged peri-ripple LC rate within 1 second preceding the ripple onset (Figure 3F, see Methods for details). Because high-quality recordings from the LC in behaving rats are technically challenging and relatively rare, we included all valid sessions in this study. The average MI, calculated per animal and per session, fell within a consistent range despite variability in the number of recording sessions (2–8 sessions per rat) across (Supplementary Figure 3). On average, LC activity significantly decreased 1.41 ± 0.06 sec (range: 1.02 – 1.88 sec) before the ripple onset and returned to the baseline after 1.70 ± 0.08 sec (range: 1.10 – 2.58 sec). Notably, maximal LC activity suppression occurred approximately 200 ms before the ripple onset (0.24 ± 0.04 sec; range: 0.03 – 0.73 sec). For all 20 datasets, the MI exceeded a 95% confidence interval (CI) of the MIs calculated around the shuffled time series, confirming a substantial decrease in LC activity around ripples.

Differential LC modulation across ripple subsets

The overall transient suppression of LC activity around hippocampal ripples, reported above, does not preclude differential LC modulation depending on ripple subtype. We therefore examined potential heterogeneity in LC modulation within a ± 6-sec time window around ripples. To this end, we randomly selected 20% of ripples from each dataset, calculated the subset modulation index (subMI) for this subset, and repeated the procedure to generate 5000 ripple subsets (537.6 ± 53.0 ripples per subset). SubMI values showed substantial variability across subsets (range: –45.70 to 1.38 a.u.; Figure 4A). On average, more than half of the subsets (65.99 ± 7.08%) exhibited significant peri-ripple LC modulation (subMI >95% CI), whereas the change of LC activity in the remaining subsets did not exceed 95% CI. Importantly, ripple intrinsic properties did not account for this variability: no significant differences were found in peak amplitude (Wilcoxon signed-rank test, Z = 0.63, p = 0.53), duration (Z = –0.52, p = 0.60), or ripple oscillation frequency (Z = 1.47, p = 0.14) between ripples in the 10th and 90th percentiles of the subMI distribution.

Instead, differences in the ongoing cortical state appeared to underlie the variability in LC modulation. The EEG preceding ripples, which were not associated with LC modulation, had a significantly higher delta (1-4 Hz) power (Wilcoxon signed-rank test, Z = –2.576, p = 0.01; Figures 4B) and enhanced spindle (10-16 Hz) power (Z = –1.829, p = 0.0674; Figures 4C), both indicating a more synchronized cortical state.

Peri-ripple LC modulation depends on the cortical-hippocampal interaction

Building on our findings, we predicted that the LC-ripple interactions might vary with arousal. Using a previously established sleep scoring procedure (Novitskaya et al., 2016; Yang et al., 2019) (Supplementary Figure 4), we classified rat behavior as awake (37.4% ± 2.9% of total recording time), NREM sleep (53.1% ± 3.2%), or REM sleep (1.2% ± 0.9%). Since ripples were extremely rare or essentially absent during REM sleep, we limited further analysis to ripples occurring during awake (awRipple) or NREM sleep (NREM-Ripple). Expectedly, LC activity was

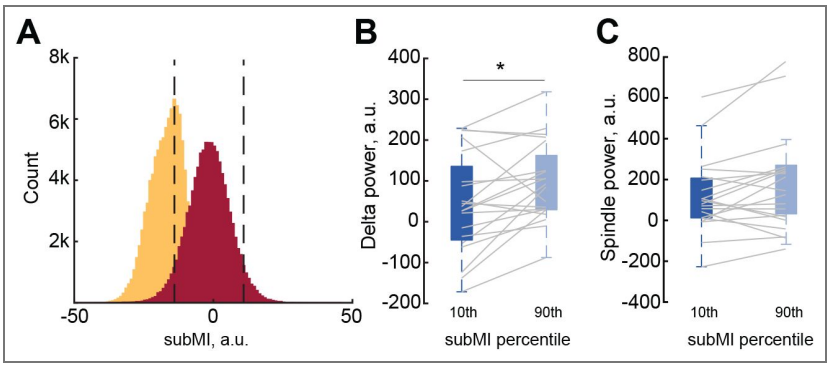

Figure 4. Differential LC modulation across ripple subsets.

(A) Distribution of modulation index (MI) values for different subsets of ripples (subMI). SubMIs were computed from the peri-event histograms of LC-MUA aligned to the ripple peak (yellow) or shuffled time series (red) for each of 5000 subsets of ripples. Vertical dashed lines indicate the 95% confidence interval (CI) boundaries for the shuffled time series. **(B, C)** The EEG delta **(B)** and spindle **(C)** power preceding 1 sec the ripple onset plotted for ripple subsets associated with different degrees of LC modulation. Box-whisker plots show the median, the 1st and 3rd quartiles, and min/max for the 10th (dark blue) and 90th (light blue) percentiles of the subMI distribution, associated with maximal and minimal LC modulation, respectively. Gray lines show data from individual rats. * $p < .05$ (Wilcoxon signed-rank test). Note a higher EEG delta power preceding ripples, associated with weak or absent LC modulation.

overall higher during awake than during NREM sleep (Figure 5A). The LC suppression occurred around both awRipples and NREM-Ripples, although the dynamic range was bigger during wakefulness. Moreover, during awRipples, LC activity did not decrease to the levels observed during NREM sleep (Figure 5A). Furthermore, peri-ripple LC modulation occurred at slower and faster temporal scales, regardless of the behavioral state. Figure 5B illustrates a slow downward drift in the LC firing rate preceding ripples, likely reflecting the ongoing brain state, as described in the previous Results section. In contrast, event-specific LC modulation had faster dynamics (Figure 5B, highlighted interval). To minimize the influence of global state fluctuations and emphasize event-related dynamics, we applied state correction and z-score normalization for further analysis.

For each data set and each behavioral state, we extracted the percent of ripple subsets with significant LC modulation (subMI >95% CI). We then correlated the subMIs with the total time spent in each behavioral state. The time spent awake, but not in NREM sleep, was significantly correlated with the proportion of ripples associated with LC suppression ($r = 0.48$, $p = 0.03$), indicating a more consistent LC modulation around awRipples.

We also examined whether differential peri-ripple LC profiles are related to ripple-spindle temporal coupling, which is known to occur during NREM sleep (Molle et al., 2006). We detected sleep spindles (504.5 ± 57.5 per session) occurring at a rate of 8.4 ± 0.8 spindles per minute and split NREM-Ripples into spindle-coupled (spRipple) and isolated (isoRipple). Next, we compared the modulation of the LC around three subtypes of ripples: awRipple (30.1% ± 3.6% of all detected ripples), spRipple (17.2% ± 1.9%), and isoRipple (48.6% ± 3.4%). The ripple subtypes differed in the intra-ripple frequency (Friedman test, $\chi 2 = 35.62$, $p < 0.0001$, post hoc pairwise comparisons were performed using Wilcoxon signed-rank tests with Holm–Bonferroni correction for multiple comparisons. awRipple vs isoRipple: $p = 0.00003$ awRipple vs spRipple: $p = 0.00004$ isoRipple vs spRipple: $p = 0.0002$), with awRipples being the fastest and spRipples the slowest (Figure 6A). There was no difference in the ripple peak amplitude (Friedman test, $\chi 2 = 3.7$, $p = 0.16$; Figure 6B). Comparison of the peri-ripple LC MUA rates across three ripple subtypes revealed a significant difference in the proportion of cases showing LC modulation (MI > 95%CI). Specifically, a significant decrease in the LC MUA was detected around awRipples in all 20 sessions (Figure 6C, left), whereas around isoRipples and spRipples, a significant change in LC-MUA was present in 13 (65%) and 4 (20%) sessions, respectively (Figure 6C). This observation was further supported by higher MI values for awRipples, intermediate MIs for isoRipples, and lowest MIs for spRipples (Figure 6D).

Due to the overall very weak or absent LC modulation around spRipples, we compared the LC MUA dynamics around awRipples and isoRipples and only in the sessions showing MI > 95% CI (Figure 6E). This analysis revealed that the onset of the LC spiking suppression occurred significantly earlier preceding awRipples (Wilcoxon signed-rank test, $Z = -2.83$, $p = 0.005$; Figure 6F) and the LC suppression was more sustained ($Z = -2.80$, $p = 0.005$; Figure 6G).

Thus, the peri-ripple LC modulation depended on the cortical-hippocampal functional connectivity, with LC activity being preserved during the periods of hippocampal-cortical communication, as indicated by the ripple-spindle coupling.

LC activity modulation around sleep spindles

Consistent with previous studies (Aston-Jones and Bloom, 1981; Swift et al., 2018), we observed LC activity modulation around sleep spindles. As expected, both spindle and LC activity were cortical state-dependent (Figure 7A). The correlation analysis confirmed that a higher spindle rate occurred during the EEG epochs with higher SI $r = 0.28$ to 0.70, $p < 0.0001$ for all sessions with highest $p = 0.00005$), Figure 7B, whereas LC-MUA and SI were anticorrelated ($r = -0.56$ to -0.21, $p < 0.01$ for all sessions with the highest $p = 0.005$, Figure 7B). LC-MUA around sleep spindles exhibited bidirectional modulation, characterized by a gradual decrease before spindle onset, followed by a rapid overshoot (Figure 7C, gray line). Similar to peri-ripple LC suppression, a relatively slow (multisecond) temporal profile likely reflected a shift in the thalamo

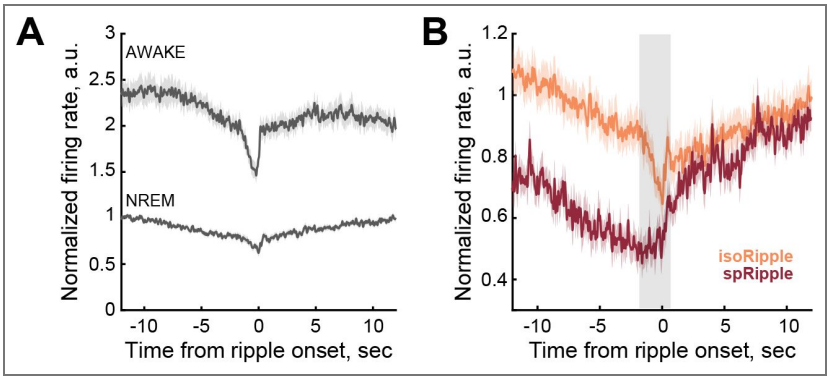

Figure 5. LC modulation around sleep oscillations.

(A) Peri-ripple LC-MUA during awake state and NREM sleep. LC activity and the range of peri-event LC modulation differed across behavioral states; it was overall higher preceding ripples occurring in wakefulness than in NREM sleep. Despite the state-dependent differences in the firing rate, peri-ripple LC modulation was observed in each behavioral state. During wakefulness, LC activity did not decrease to the levels observed during NREM sleep. **(B)** Peri-event LC-MUA around isolated and spindle-coupled ripples during NREM sleep. LC activity exhibited fast peri-ripple dynamics (highlighted interval) superimposed on slower, state-dependent fluctuations around isolated ripples. Fast LC modulation was absent, while slow fluctuations were preserved around ripples coupled with sleep spindles. For all plots, LC-MUA firing rate was scaled to a pre-event baseline interval [−12 to −10 sec] to preserve baseline differences in LC activity across behavioral states. Bin size: 50 ms. isoRipple – isolated ripple, spRipple -spindle-coupled ripple.

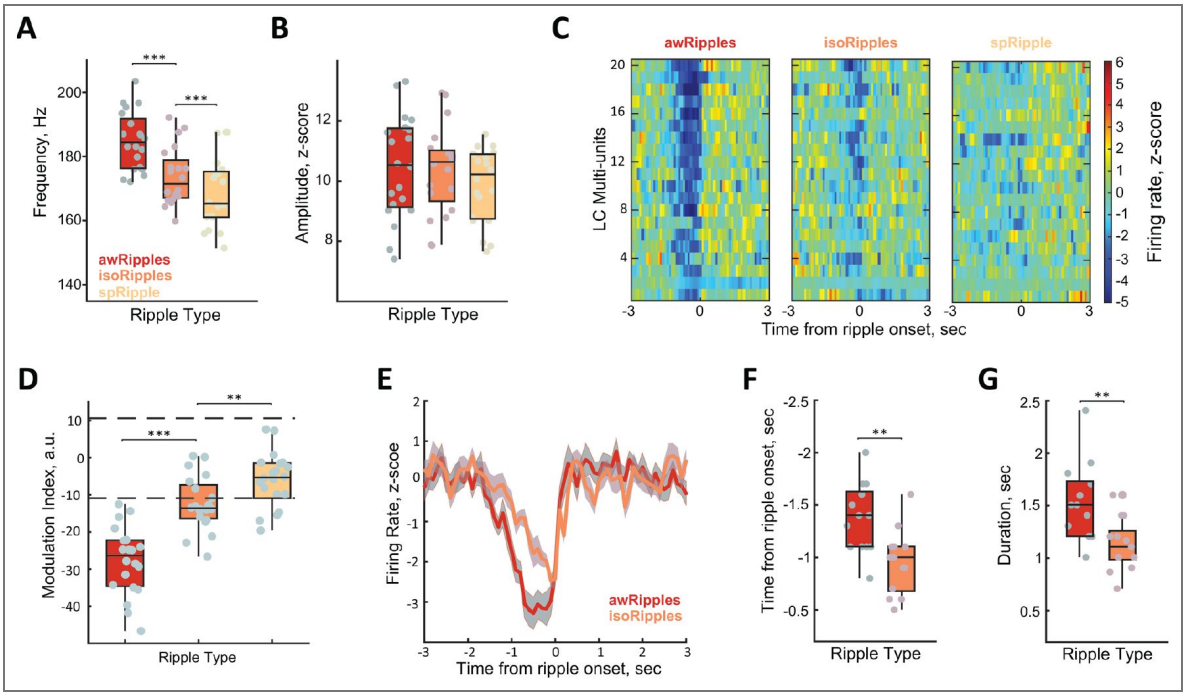

Figure 6. State-dependent modulation of LC activity across ripple subtypes.

(A, B) Intra-ripple frequency and peak amplitude **(B)** for different ripple types. Box-whisker plots show the median, the 1st and 3rd quartiles, and min/max. Gray dots show data from individual rats. *** - $p < 0.001$ for post hoc pairwise comparisons (Wilcoxon signed-rank tests with Holm–Bonferroni correction for multiple comparisons). **(C, D)** Differential LC activity modulation across ripple types. Session-averaged LC multi-unit activity (MUA) aligned to the ripple onset **(C)** and MI **(D)** is shown for different ripple types. The LC MUA rate is color-coded and plotted for individual sessions. Note the strongest LC activity suppression around ripples occurring in wakefulness (awRipples) and the weakest around ripples coupled with sleep spindles (spRipples). **(E-G)** The patterns of LC activity around different ripple types. The temporal dynamics **(E)**, the onset **(F)**, and the duration **(G)** of ripple-associated LC MUA modulation are shown for ripples occurring during awake (awRipples) and NREM sleep (isoRipples). The data from sessions with significant LC MUA rate decreases are shown. Note an earlier onset and longer duration of LC activity modulation around awake ripples. Due to an overall weak or absent LC activity modulation, data from spindle-coupled ripples are not shown.

-cortical network preceding sleep spindles. We generated shuffled time series and did not observe any significant LC modulation (not shown). To isolate the LC activity pattern that is not state-dependent, we subtracted LC-MUA aligned to shuffled time series from LC-MUA aligned to spindle onsets. This procedure refined the time window of a transient LC-MUA change (Figure 7C, brown line). Specifically, LC-MUA exhibited a sharp decrease 2.5 ± 0.09 s before spindle onset, followed by a rapid return to baseline and a small overshoot roughly corresponding to the duration of a sleep spindle (1.1 to 2.8 s). Overall, a significant LC modulation (MI > 95% CI) around sleep spindles was present in 17 out of 20 sessions (Figure 7D).

We next explored if the temporal profile of spindle-associated LC-MUA differed around ripple-coupled (ripSpindle, 41.3 ± 3.1% of all detected spindles) and ripple-uncoupled (isoSpindle, 58.7 ± 3.1%) spindles. Notably, isoSpindles were significantly shorter compared to ripSpindles (1.32 ± 0.05 sec and 1.51 ± 0.06 sec, respectively; Z = –3.92, p = 0.000089; Figure 7E), but two subtypes of sleep spindles did not differ in their oscillatory frequency (ripSpindle: 15.37 ± 0.11 Hz, isoSpindle: 15.33 ± 0.09 Hz; Wilcoxon signed-rank test, Z = –0.22, p = 0.82) or maximum power (ripSpindle: 1.98 ± 0.14 a.u., isoSpindle: 2.08 ± 0.15 a.u.; Z = 1.27, p = 0.20). Despite visible differences in the dynamics of z-scored LC MUA around two types of spindles (Figure 7F), the absolute LC-MUA rate, nor SI differed during a 2-sec time window preceding either group of spindles (Kolmogorov-Smirnov test, p > 0.05 for both variables and all sessions, not shown). Across sessions, MI values exceeded 95% CI in 17/20 datasets for isoSpindles and only 3/20 for ripSpindles. Thus, LC modulation was more consistent and pronounced around isoSpindles compared to ripSpindles (Figures 7F and 7G). Together, this result provided further evidence that LC activity is preserved during hippocampal–cortical communication, as reflected by ripple–spindle coupling.

Lastly, the detection of coupled events (spRipple and ripSpindle) was performed independently, although some overlap cannot be excluded. Supplementary Figure 5 shows a significant correlation (Pearson r = 0.72, p = 0.0003) between the MI around spRipples and ripSpindles. Overall, we found that LC suppression was generally weak around both types of coupled events. Specifically, session-averaged spRipple-associated LC suppression reached a significance level (exceeding 95% CI) in 4 (n = 3 rats) out of 20 sessions. The significant ripSpindle-associated LC suppression was observed in 3 (n = 2 animals) out of 20 sessions.

Discussion

Using multi-site electrophysiology in freely behaving adult male rats, we characterized the dynamics of LC neuronal activity and hippocampal ripples across two temporal scales. Both LC firing and ripple occurrence were strongly state-dependent, yet inversely related: periods of heightened arousal were marked by increased LC activity and reduced ripple rates. At a finer temporal resolution, LC spiking consistently decreased approximately 1–2 seconds before ripple onset. The magnitude of peri-ripple LC modulation varied across ripple subsets but was not correlated with ripple intrinsic properties. Notably, the strongest LC modulation occurred around ripples in the awake state, whereas LC activity remained largely unchanged around ripples coupled with sleep spindles during NREM sleep. Together, these findings provide novel insight into the state-dependent dynamics of cross-regional interactions and highlight the LC as a key component of a large-scale cortical–subcortical network supporting offline information processing.

LC-NE dynamics during NREM sleep and its functional implications

LC activity has long been established to fluctuate with arousal level; it is higher during vigilant states and lower during sleep (Aston-Jones and Bloom, 1981). This pioneering work has promoted extensive research that has established the critical engagement of the LC-NE system in many cognitive functions dependent on real-time processing of incoming information (Berridge and Waterhouse, 2003; Sara and Bouret, 2012; Sara, 2009). However, only recently has the field begun to uncover the temporal dynamics of LC-NE activity and its functional significance during states of low vigilance, such as NREM sleep. Using opto- and chemogenetic tools, it has been confirmed that LC activation induces awakening, whereas LC inhibition promotes sleep (Carter et

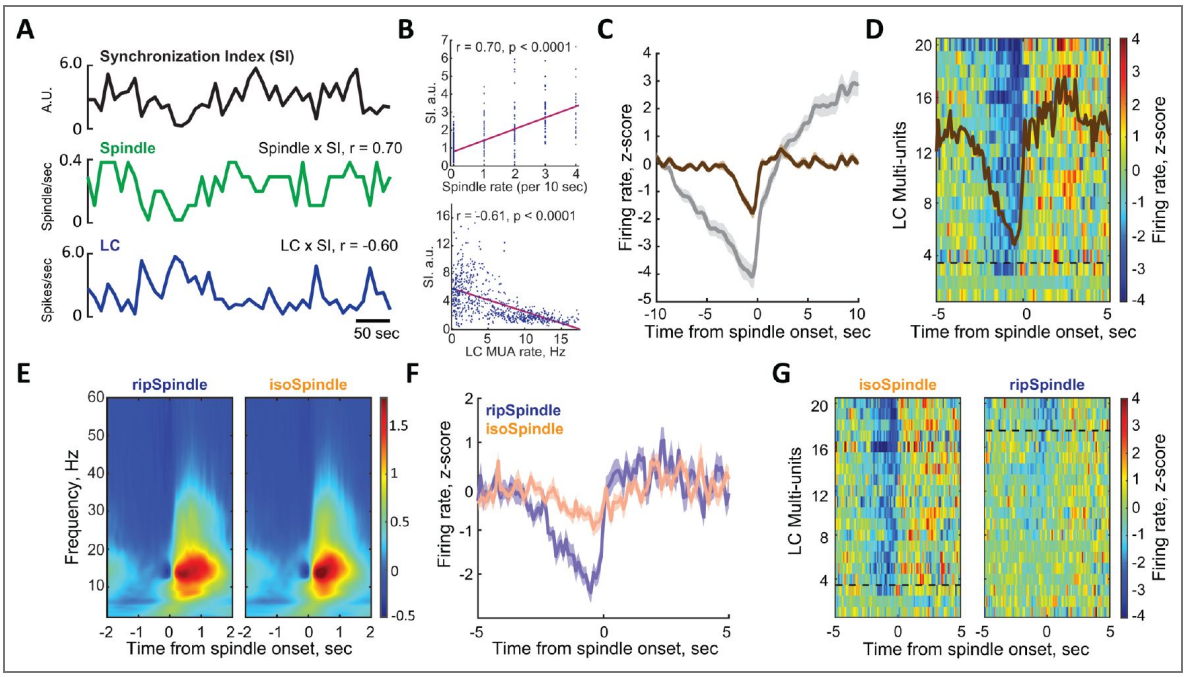

Figure 7. LC activity modulation around sleep spindles.

(A) Representative traces illustrating the relationship between cortical state, assessed by the Synchronization Index (SI), LC multiunit activity (LC-MUA), and sleep spindle rate. **(B)** Correlation of LC-MUA rate with SI (upper panel) and spindle rate (lower panel) from a representative session. **(C–D)** Spindle-associated LC modulation across slower and faster temporal scales. **(C)** A decrease in LC firing rate was observed as early as 10 s before the spindle onset (gray line). This slow LC modulation was likely driven by fluctuations in ongoing cortical state. To reduce the state-dependent effect, LC-MUA aligned to shuffled spindle times was subtracted. The resulting state-corrected LC-MUA trace (brown) revealed faster LC dynamics. LC-MUA was averaged and smoothed using a 1 Hz low-pass filter. **(D)** Color-coded LC-MUA (state-corrected and z-scored) aligned to the spindle onset for each dataset, with the overlay representing the grand average across sessions (n = 20). **(E)** EEG spectrograms around ripple-coupled (ripSpindle) and isolated (isoSpindle) sleep spindles. The ripSpindle was detected if at least one ripple occurred between the spindle on/offset. Spindle duration was extracted as the time between the spindle on/offset. The ripSpindles were significantly longer (Wilcoxon signed-rank test, $p < 0.0001$, see Results for more details). **(F–G)** LC activity profiles around ripSpindles and isoSpindles, shown as the grand average **(F)** and session-averaged responses **(G)**. Dashed lines in **(D)** and **(G)** separate cases with significant (top) and non-significant LC modulation.

al., 2010; Vazey and Aston-Jones, 2014). Consistent with earlier studies, we observed cortical state-dependent fluctuation of LC neuronal activity in naturally behaving rats. By quantifying cortical state dynamics during NREM sleep at a 4-s resolution, we found an inverse correlation between the LC firing rate and the degree of cortical arousal as indicated by SI. Furthermore, LC activity during NREM sleep was inversely correlated with the incidence of hippocampal ripples and sleep spindles; the latter result is in agreement with inverse relationships between NE release and the power of spindle oscillations (Osorio-Forero et al., 2021). Collectively, these observations suggest the existence of a large-scale coordinated network regulating the NREM sleep microstructure and possibly mediating offline information processing.

In our earlier study, by recording LC spiking activity in naturally behaving rats, we observed a delayed time window of enhanced LC neuron firing, specifically during NREM sleep episodes after learning (Eschenko and Sara, 2008). Recent studies in mice uncovered infra-slow (~0.02 Hz) fluctuations of cortical and thalamic NE release during NREM sleep and related the LC activity dynamics to the regulation of sleep microstructure and state transitions (Osorio-Forero et al., 2021; Kjaerby et al., 2022). Furthermore, optogenetic LC stimulation at 2Hz during NREM sleep after exposure to a spatial memory task, whilst not affecting ripple occurrence, decreased the stability of replay of hippocampal place cells and caused a memory deficit (Swift et al., 2018). This finding aligns with our previous results demonstrating that phasic LC activation time-locked to ripples during post-learning sleep disrupts spatial memory consolidation (Novitskaya et al., 2016).

While the mechanisms and functional significance of LC activity patterns during NREM sleep remain to be fully understood (Foustoukos and Lüthi, 2025; Sara, 2017; Poe, 2017), these observations align with pharmacological evidence showing that experimental manipulation of NE transmission following learning can alter memory strength (Przybyslawski et al., 1999; Sara et al., 1999; Roullet and Sara, 1998; Miranda et al., 2009; Gibbs et al., 2010; Gazarini et al., 2013; Gais et al., 2011). Our recent work suggested a potential network mechanism by which the LC–NE system contributes to sleep-dependent memory consolidation (Duran et al., 2023). Specifically, we demonstrated that both $\alpha 2$- and β-adrenoceptors are involved in the generation of hippocampal ripples. Moreover, pharmacological manipulation of noradrenergic transmission after learning altered all major NREM sleep oscillations and their coupling, potentially leading to less efficient spatial memory consolidation (Duran et al., 2023). The present findings extend this work by providing new insights into how LC neuronal activity contributes to the expression of normal sleep microarchitecture.

Coerulear-hippocampal interactions for memory consolidation

Hippocampal ripples are broadly recognized as a central mechanism of memory consolidation (Klinzing et al., 2019; Skelin et al., 2018). Emerging work has begun to reveal the circuit mechanisms by which hippocampal ripples engage a larger brain network that includes the prefrontal cortex, thalamus, amygdala, and ventral tegmental area (VTA) for offline information processing (Girardeau et al., 2017; Latchoumane et al., 2017; Gomperts et al., 2015; Wang and Ikemoto, 2016; Yang et al., 2019). Our findings expand this memory-supporting circuit to the LC-NE system. By characterizing LC and hippocampal activity at a fine temporal scale, we revealed differential patterns of coerulear-hippocampal interactions. First, we observed consistent transient suppression of LC activity occurring 1-2 seconds before the ripple onset. This cessation of LC neuron spiking and the corresponding depletion of NE might have enabled a network to shift to a transient state of enhanced synchronization, allowing ripple generation. This view is indirectly supported by an increase in the EEG delta power immediately preceding the ripple onset, when LC activity is suppressed.

Second, we showed that the degree of LC modulation varied across different subsets of ripples. The strongest and most consistent peri-ripple LC inhibition was observed during the awake state. Interestingly, ripples occurring during wakefulness have been associated with stronger and more structured neuron ensemble reactivation, which was correlated with recent experience (Tang et al., 2017). Therefore, a transient silence of LC might be beneficial for the ripple-associated

reactivation of recent memory traces. Similarly, coordinated activity of reward-related VTA neurons was greater around ripples that were associated with reactivation of neuronal ensembles that relayed recent learning experience (Gomperts et al., 2015). Conversely, LC activation induces arousal, shifts the network to a state incompatible with ripple generation, and thereby might cause interference for the consolidation of recently acquired information (Novitskaya et al., 2016; Swift et al., 2018).

During NREM sleep, despite substantially reduced LC activity, we observed a fine-tuned LC activity dynamics around ripples. Specifically, LC neuron discharge was only mildly reduced around isolated ripples, and it was largely preserved during ripples co-occurring with sleep spindles. Differential firing patterns for spindle-coupled and -uncoupled ripples have been reported for cortical and thalamic neurons (Peyrache et al., 2011; Varela et al., 2001; Yang et al., 2019). During NREM sleep, hippocampal ripples occur in coordination with cortical slow oscillations and sleep spindles (Maingret et al., 2016). The precise temporal correlation between the oscillatory patterns expressed during NREM sleep has been causally linked to memory consolidation by mediating the transfer of newly encoded information from the hippocampus to the cortex for long-term storage (Latchoumane et al., 2017; Buzsaki, 1996; Molle et al., 2006; Maingret et al., 2016; Klinzing et al., 2019).

At first glance, the suppression of LC activity around ripples that we observed in the present study may seem inconsistent with the established role of NE in facilitating ripple-mediated synaptic plasticity (Norimoto et al., 2018; Sadowski et al., 2016). Remarkably, LC activity was indeed preserved around some subsets of ripples. In our previous work, we showed that LC activation during the time windows marking hippocampal-cortical communication interferes with the cortical dynamics and is detrimental for spatial memory (Novitskaya et al., 2016).

Differential modulation of LC activity that was observed in the present study supports the idea that reduced NE release in the hippocampus might bias the content of memory trace during the subsequent ripples and weaken the reactivation of irrelevant experiences. In general, our results highlight the importance of preserved NE transmission at times of cross-regional information transfer. An overall higher LC firing rate during states of elevated arousal may require a larger dynamic range of LC activity modulation (Kjaerby et al., 2022). Therefore, in the awake state, a more pronounced suppression of LC activity may be required for the network shift permitting ripple generation.

In summary, our results demonstrate a state-dependent noradrenergic influence on the thalamocortical–hippocampal circuit and position the LC as part of an extended brain network whose coordinated activity supports system-level memory consolidation. Conducting behavioral assays before electrophysiological recordings, along with spatially and temporally precise modulation of LC activity during recording sessions, will be essential for achieving a mechanistic understanding of network dynamics and its functional role for memory consolidation in future investigations. Our present results suggest that during wakefulness, transient suppression of noradrenergic transmission might facilitate the generation of hippocampal ripples and sleep spindles by enhancing network synchrony. We propose that reduced peri-ripple LC activity during the awake state may preferentially promote the replay of recent memory traces by limiting interference from remote memories, which are more likely to be reactivated in more alert states. In contrast, during NREM sleep, preserved LC activity during ripples coinciding with sleep spindles suggests a role for NE in facilitating cross-regional communication underlying memory-related information transfer. These results provide new insight into how the LC–NE system shapes memory processing across brain states and open the way for future causal investigations using modern circuit-level tools.

Methods and Materials

Animals

Seven adult male Sprague-Dawley rats were used. Data from one rat has been collected for a previous study Eschenko et al.(2012) and reanalyzed. An additional six rats (Charles River Laboratory, Germany) were kept on a 12-hour light-dark cycle (8:00 am lights on) and single-housed after surgery. Recordings were performed during the dark cycle. Similar surgery and recording procedures were used as reported in detail elsewhere (Yang et al., 2019; Eschenko et al., 2012). The study was performed in accordance with the German Animal Welfare Act (TierSchG) and Animal Welfare Laboratory Animal Ordinance (TierSchVersV). This is in full compliance with the guidelines of the EU Directive on the protection of animals used for scientific purposes (2010/63/EU). The study was reviewed by the ethics commission (§15 TierSchG) and approved by the state authority (Regierungspräsidium, Tübingen, Baden-Württemberg, Germany).

Surgery and electrode placement

Procedures for stereotaxic surgery under isoflurane anesthesia have been described in detail elsewhere (Yang et al., 2019). Briefly, anesthesia was initiated with 4% and maintained with 1.5-2.0% isoflurane. Body temperature, heart rate, and blood oxygenation were monitored throughout the entire anesthesia period. The depth of anesthesia was controlled by a lack of pain and sensory response (hind paw pinch). A fully anesthetized rat was fixed in a stereotaxic frame with the head angle at zero degrees. The skull was exposed and a local anesthetic (Lidocard 2%, B. Braun, Melsungen, Germany) was applied to the skin edges. Craniotomies were performed on the right hemisphere above the target regions. Additional burr holes were made for EEG, grown, and anchor screws (stainless steel, 0.86-1.19 mm diameter, Fine Science Tools, Heidelberg, Germany). Dura mater was removed when necessary. For extracellular recording, single platinum-iridium electrodes (FHC, Bowdoin, ME) were placed in the anterior cingulate cortex (ACC, AP/ML: 2.8 mm/0.8mm from Bregma and DV: 1.8 mm from the dura surface). For the recording of the hippocampal ripples, the electrode was mounted on a self-made movable microdrive and inserted above the CA1 subfield of the dorsal hippocampus (dHPC, -3mm/2mm/ 2mm). For LC recordings, single platinum–iridium electrodes (FHC, Bowdoin, ME; n = 1), microwire brush electrodes (Micro-Probes, MD; n = 2), and silicon probes (Cambridge Neurotech, Cambridge, UK; n = 2) were mounted on a microdrive (Cambridge Neurotech, Cambridge, UK) and implanted above the LC (4.2 mm posterior, 1.2 mm lateral from lambda; DV: 5.5–6.2 mm) at a 15° angle. We also implanted one rat with a polymer electrode array (LLNL, Livermore, CA). The accuracy of LC targeting was verified by online monitoring of neural activity. The LC neurons were identified by broad spike widths (0.6 msec), regular low firing rate (1 –2 spikes/s), and a biphasic (excitation followed by inhibition) response to paw pinch. For EEG recording, a screw was placed above the frontal cortex. The ground screw was placed above the cerebellum. Screws were fixed in the skull and additionally secured with tissue adhesive. The entire implant was secured on the skull with dental cement (RelyX™ Unicem 2 Automix, 3M, MN). A copper mesh was mounted around the implant for shielding and protection of exposed connection wires. During the post-surgery recovery period, analgesic (2.5 mg/kg, s.c.; Rimadyl, Zoetis) and antibiotic (5.0 mg/kg, s.c.; Baytril®) were given for 3 and 5 days, respectively. Electrode placements were histologically verified.

Electrophysiological recording and data analysis

Rats were first habituated to the sleeping box (30 × 30 × 40 cm) and the cable plugging procedure. The electrodes were either connected to the Neuralynx Digital Lynx or FreeLynx wireless acquisition system via two 32-channel head stages (Neuralynx, Bozeman, MT). The electrode placement in the LC was optimized by lowering the electrodes with a maximal 0.05 mm step and monitoring spiking activity on the high-passed (300 Hz – 8kHz) extracellular signal. The depth of the dHPC electrodes was adjusted by gradually lowering the electrode (maximum 0.05 mm per day) until reliable ripple activity was observed. Once the electrode position was optimized, the

broadband (0.1Hz - 8kHz) extracellular signals were acquired and digitized at 32kHz and referenced to the ground screw. The animals' movement was monitored by an EMG electrode attached to the neck muscle. All recordings were performed between 10 a.m. and 7 p.m.

Classification of behavioral states

We classified the rat's spontaneous behavior into awake and NREM sleep using frontal EEG or cortical LFPs by applying a previously established sleep scoring algorithm (Novitskaya et al., 2016; Yang et al., 2019). Briefly, animal movement speed was extracted from the video recording synchronized with a neural signal. The theta/delta (θ/δ) ratio was calculated from the artifact-free EEG in 4-sec epochs. The epochs of the awake state were identified by the presence of active locomotion and above θ/δ threshold; the epochs of NREM sleep were identified by the absence of motor activity and below θ/δ threshold. The minimal duration of the same behavioral state was set to 20 sec; data segments with less steady behavioral states were excluded from further analysis.

Event detection

For detection of the hippocampal ripples, a broadband (0.1 Hz - 8 kHz) extracellular signal recorded from the dHPC (pyramidal layer, CA1 subfield) was band-pass (120 – 250 Hz) filtered, rectified, and low-pass filtered (25 Hz). The resulting signal was z-score normalized, and ripple oscillations were detected by signal thresholding at 5 standard deviations (SDs). Ascending and descending crossings at 1 SD defined the ripple onset and offset, respectively. Clustered and isolated ripples were classified based on the inter-ripple interval (IRI) as described in detail elsewhere (Selinger et al., 2007). Briefly, IRIs were extracted, and the log(IRI) distribution was analyzed. A bimodal log(IRI) distribution indicated ripple occurrence with shorter and longer IRI. A crossing point of two distributions was used for classifying the ripple type. Ripples with short IRI (< 0.33 sec) were classified as 'clustered' and treated as a single ripple event; the onset time was defined by the first ripple in a cluster. Ripples with IRI > 0.33 sec were classified as 'isolated'.

For the detection of sleep spindles, the EEG signal was band-pass (12 - 16 Hz) filtered, down-sampled (200 Hz), and the root mean square (0.2 s smoothing) was calculated. The spindle detection threshold was defined at 3 SD of the signal amplitude during NREM sleep episodes. Ascending and descending signal crossings at 1SD defined the spindle on- and offset, respectively. The spindle duration was extracted as the time between the spindle onset and offset; the minimal sleep spindle duration was set to 0.5 sec. Coupled oscillatory events were defined as ripples occurring between spindle onset and offset.

Analysis of peri-event neural activity

For analysis of LC activity modulation around ripples, we used a previously established method (Yang et al., 2019). First, the spike times of LC multiunit activity (LC-MUA) were extracted by high-pass (600Hz) filtering of the broadband extracellular signal recorded from LC and thresholding at -0.05 mV. The LC-MUA was triggered on ripple/spindle onset, and the averaged peri-event spike histogram (PETH) was generated either ± 6 sec or ± 3 sec around all detected ripples and ± 5 sec around sleep spindles (5-ms bins, Gaussian smoothed with a 10-ms window). To compensate for possible state-dependent fluctuations of LC-MUA, a 'surrogate' event sequence was generated by randomly distributing the same number of time points within a 4-second time window around each event; the jittering procedure was repeated 100 times. The averaged PETH was generated around jittered events. Time series of LC MUA around the jittered events were subtracted from the corresponding values around real events and the resulting ('corrected') PETHs were z-score normalized. To further smooth the PETH, we extracted the area above/below the curve of each PETH every 100ms and z-scored the modulation response. To quantify peri-event dynamics of LC-MUA, a modulation index (MI) was calculated by modulation response within 1 sec before the event onsets. To determine the significance of modulation, we calculated the modulation responses around 'shuffled' ripple times generated by permutation of the IRIs and calculated the MIs for each of the 5000 shuffled PETHs; a 95% confidence interval (CI) served as

the significance threshold. To quantify the LC-MUA modulation around subsets of ripples, subsampled MI (s-MI) was computed for a subset of ripples (20% of all detected ripples in each session), and the same procedure was repeated 5000 times. The s-MI distribution was analyzed.

Spectral analysis

For LFP analysis, we applied the Morlet-wavelet time-frequency analysis to estimate spectral power around ripple onsets. To compare delta and spindle band activity preceding ripples associated with either strong or weak LC activity modulation, we first averaged the spectral power within the delta (1–4 Hz) and spindle (12–16 Hz) frequency bands over a 2-s window before ripple onset. We then quantified the power by calculating the area under the curve for each frequency band.

Statistical Analysis

All statistical analyses were performed in MATLAB (MathWorks, Natick, MA). The analysis of variance (one-way ANOVA) or the Kolmogorov–Smirnov test was used for between-group comparisons, with significance defined as $p < 0.05$. The Wilcoxon signed-rank test was used to compare two matched samples. The Friedman test was used to compare intrinsic ripple properties. Post hoc analyses were performed using the Wilcoxon signed-rank test with Holm–Bonferroni correction for multiple comparisons ($p < 0.05$ after correction). Pearson correlation was used to assess relationships between variables, with significance defined as $p < 0.05$.

Data availability

Data will be available upon request.

Supplementary figures

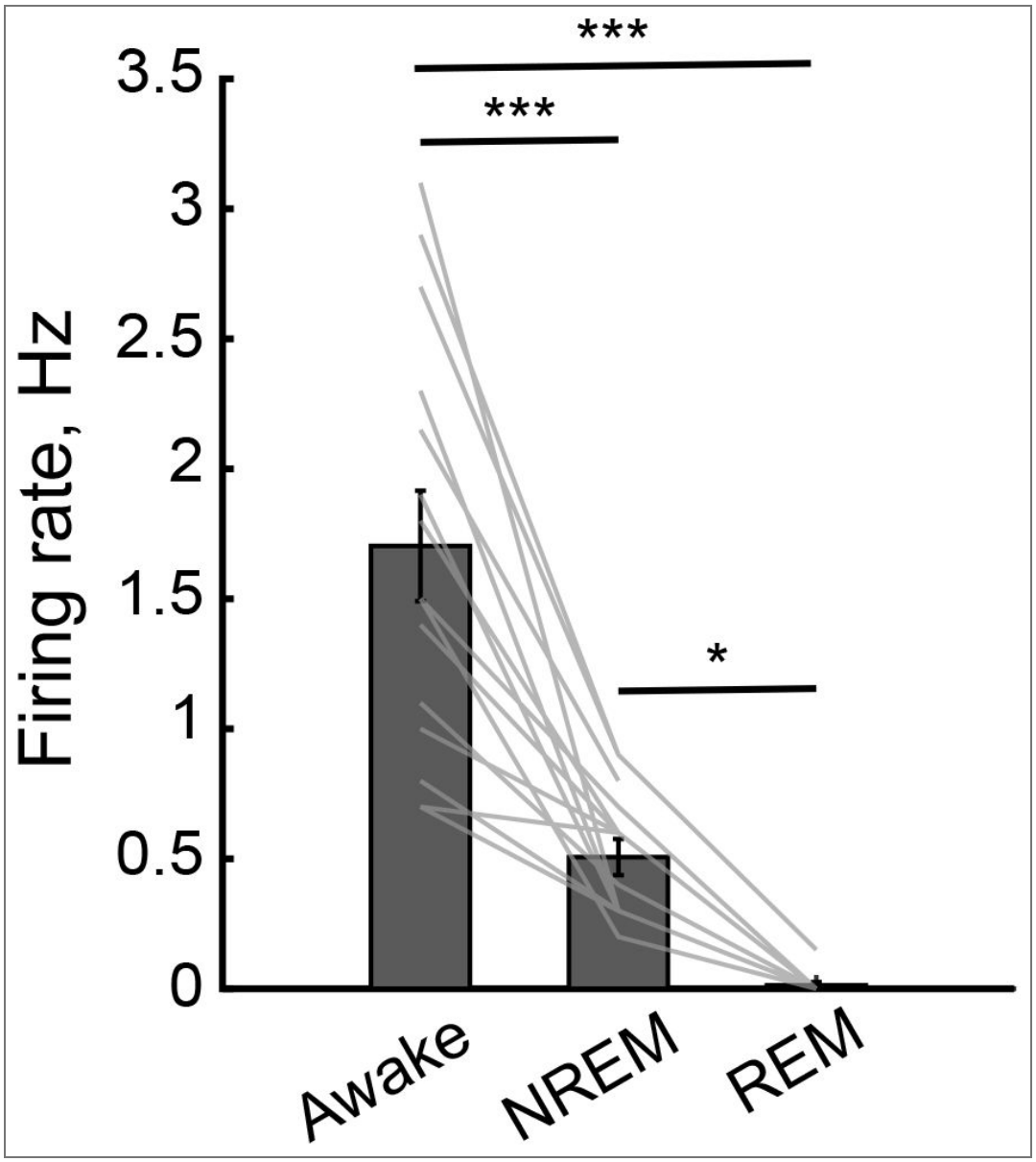

Supplementary figure 1. Firing rates of LC neurons across sleep/awake states. Bars show the grand means (± SE) and gray lines show session-averages for each rat. * $p < 0.05$, ** $p < 0.01$, and *** $p < 0.001$ (one-way ANOVA).

Supplementary figure 2. **Slow-timescale modulation of ripple-associated LC activity.**

The LC firing rate (blue trace; bin size: 0.05 s) is plotted ±12 s around ripple onset for a representative session. Notably, a decrease in LC firing rate emerges as early as 10 s prior to ripple onset.

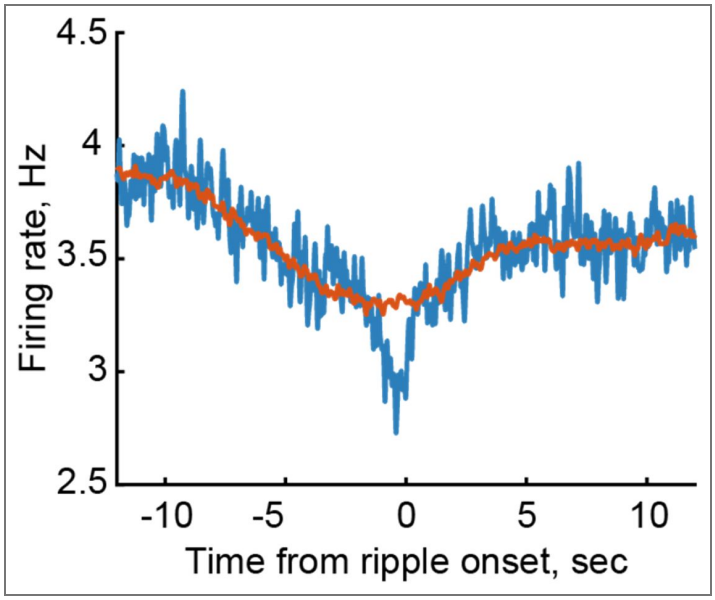

Supplementary figure 3. **Distribution of the modulation index (MI) across rats and sessions.**

(A) The average MI is shown for each animal, with rat ID and number of sessions indicated in parentheses. Dashed lines denote the mean ± 2 standard deviations across all sessions. Animal-averaged MIs fall within a consistent range, indicating that the distribution is not driven by a single subject (e.g., rat 1101, 8 sessions). **(B)** The average MI is shown for each session. The eight sessions from rat 1101 are indicated by gray-filled triangles. Comparison of these sessions with the remaining 12 sessions from six other animals revealed no significant difference in MI distribution (Kolmogorov–Smirnov test, p = 0.969).

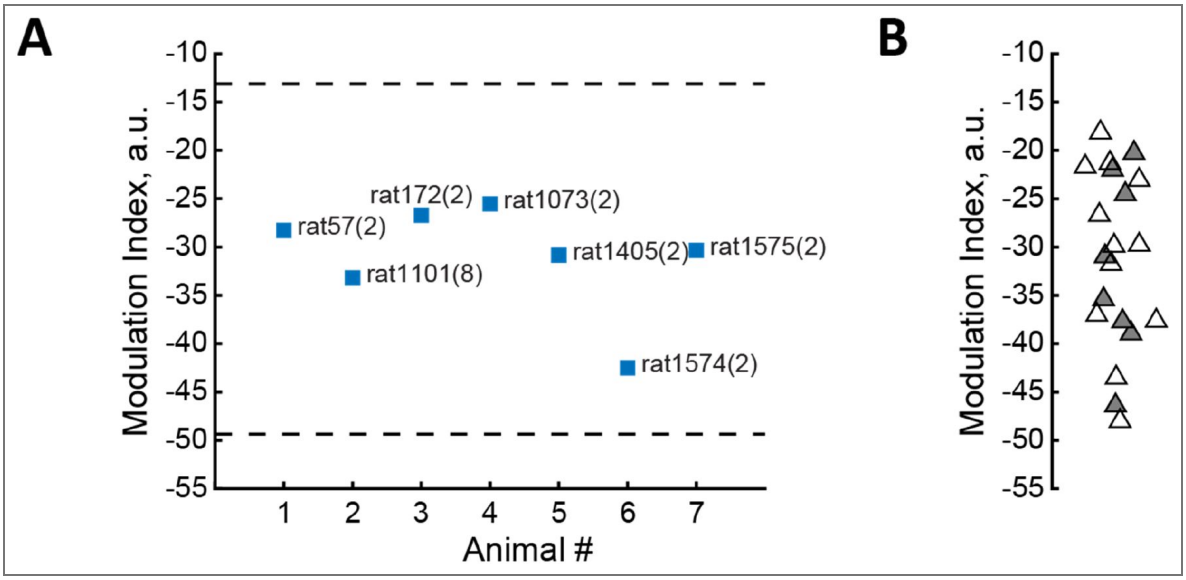

Supplementary figure 4. **Sleep scoring procedure.Classified NREM sleep and wake episodes (top), with corresponding raw EEG traces (1–300 Hz; middle) and Synchronization Index (SI; bottom), calculated over 4-s epochs.**

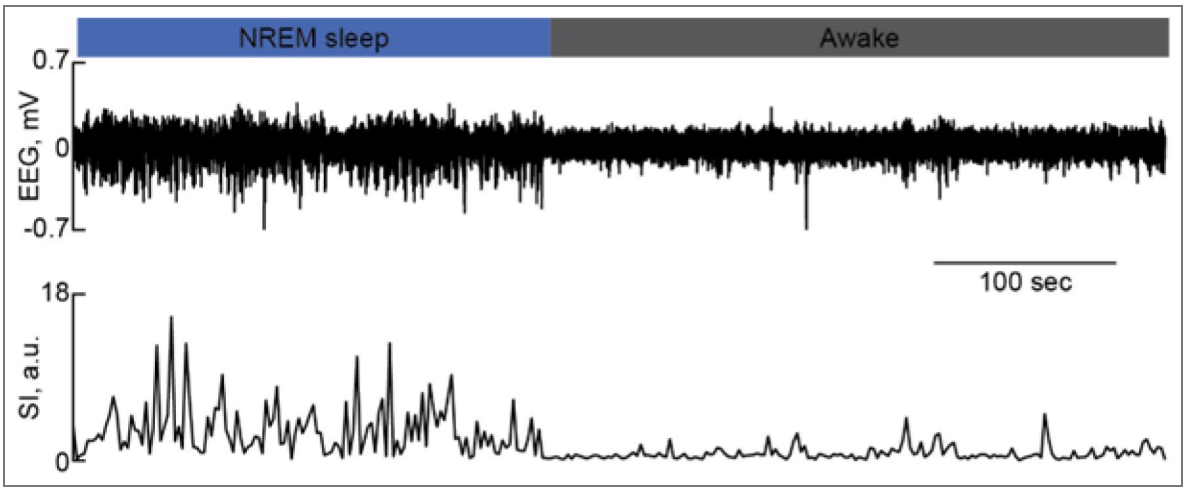

Supplementary figure 5. **LC modulation around coupled oscillations.**

Pearson correlation between the modulation index (MI) for spindle-coupled ripples (spRipple) and ripple-coupled spindles (ripSpindle). Detection of coupled oscillations (spRipple and ripSpindle) was performed independently, although some overlap cannot be excluded. Blue square highlights three sessions exhibiting significant (MI < 95% CI) LC suppression around both ripSpindles and spRipples. Generally, LC modulation around coupled oscillations was weak. Specifically, the LC suppression around spRipples and ripSpindles reached significance in 4 sessions (from 3 rats) and 3 sessions (from 2 rats), respectively, out of a total of 20 sessions (from 7 rats).

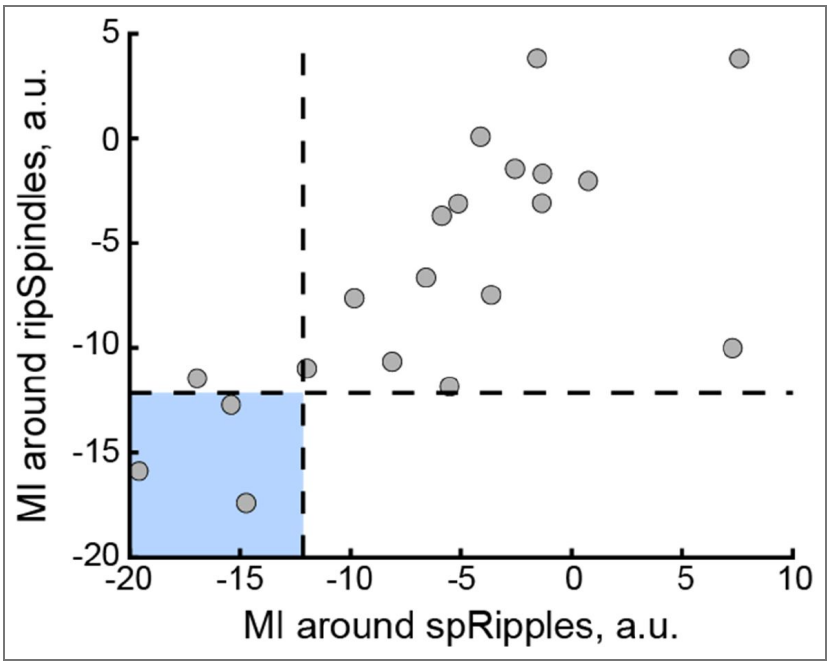

Acknowledgements

We thank Axel Oeltermann and Joachim Werner for their technical support.

Additional information

Funding

Funder	Grant reference number	Author
Max-Planck-Gesellschaft (MPG)		Mingyu Yang Oxana Eschenko

Author ORCID iDs

Oxana Eschenko: https://orcid.org/0000-0001-7482-5628

References

Aston-Jones G, Bloom FE (1981) Activity of norepinephrine-containing locus coeruleus neurons in behaving rats anticipates fluctuations in the sleep-waking cycle. *J Neurosci* **1**:876-86 https://doi.org/10.1523/jneurosci.01-08-00876.1981 | PubMed

Berridge CW, Waterhouse BD (2003) The locus coeruleus-noradrenergic system: modulation of behavioral state and state-dependent cognitive processes. *Brain Res Brain Res Rev* **42**:33-84 https://doi.org/10.1016/s0165-0173(03)00143-7 | PubMed

Brodt S, Inostroza M, Niethard N, Born J. (2023) Sleep-A brain-state serving systems memory consolidation. *Neuron* **111**:1050-1075 https://doi.org/10.1016/j.neuron.2023.03.005 | PubMed

Buzsaki G. (1996) The hippocampo-neocortical dialogue. *Cereb Cortex* **6**:81-92 https://doi.org/10.1093/cercor/6.2.81 | PubMed

Cahill L, Prins B, Weber M, McGaugh JL (1994) Beta-adrenergic activation and memory for emotional events. *Nature* **371** https://doi.org/10.1038/371702a0 | PubMed

Carter ME, Yizhar O, Chikahisa S, Nguyen H, Adamantidis A, Nishino S, Deisseroth K, de Lecea L. (2010) Tuning arousal with optogenetic modulation of locus coeruleus neurons. *Nat Neurosci* **13**:1526-33 PubMed | https://doi.org/10.1038/nn.2682

Clayton EC, Williams CL (2000) Noradrenergic receptor blockade of the NTS attenuates the mnemonic effects of epinephrine in an appetitive light-dark discrimination learning task. *Neurobiol Learn Mem* **74**:135-45 PubMed | https://doi.org/10.1006/nlme.1999.3946

Duran E, Pandinelli M, Logothetis NK, Eschenko O. (2023) Altered norepinephrine transmission after spatial learning impairs sleep-mediated memory consolidation in rats. *Sci Rep* **13**:4231 PubMed | https://doi.org/10.1038/s41598-023-31308-1

Eschenko O, Magri C, Panzeri S, Sara SJ (2012) Noradrenergic neurons of the locus coeruleus are phase locked to cortical up-down states during sleep. *Cereb Cortex* **22**:426-35 PubMed | https://doi.org/10.1093/cercor/bhr121

Eschenko O, Sara SJ (2008) Learning-dependent, transient increase of activity in noradrenergic neurons of locus coeruleus during slow wave sleep in the rat: brain stem-cortex interplay for memory consolidation?. *Cereb Cortex* **18**:2596-603 PubMed | https://doi.org/10.1093/cercor/bhn020

Foustoukos G, Lüthi A. (2025) Monoaminergic signaling during mammalian NREM sleep - Recent insights and next-level questions. *Curr Opin Neurobiol* **92**:103025 https://doi.org/10.1016/j.conb.2025.103025 | PubMed

Foustoukos G, Lüthi A (2025) Monoaminergic signaling during mammalian NREM sleep - Recent insights and next-level questions. *Curr Opin Neurobiol* **92**:103025 https://doi.org/10.1016/j.conb.2025.103025 | PubMed

Gais S, Rasch B, Dahmen JC, Sara S, Born J. (2011) The Memory Function of Noradrenergic Activity in Non-REM Sleep. *Journal of Cognitive Neuroscience* **23**:2582-2592 https://doi.org/10.1162/jocn.2011.21622 | PubMed

Galeotti N, Bartolini A, Ghelardini C. (2004) Alpha-2 agonist-induced memory impairment is mediated by the alpha-2A-adrenoceptor subtype. *Behavioural Brain Research* **153**:409-417 https://doi.org/10.1016/j.bbr.2003.12.016 | PubMed

Gazarini L, Stern CAJ, Carobrez AP, Bertoglio LJ (2013) Enhanced noradrenergic activity potentiates fear memory consolidation and reconsolidation by differentially recruiting α1- and β-adrenergic receptors. *Learning & Memory* **20**:210-219 https://doi.org/10.1101/lm.030007.112 | PubMed

Gelinas JN, Nguyen PV (2005) β-Adrenergic Receptor Activation Facilitates Induction of a Protein Synthesis-Dependent Late Phase of Long-Term Potentiation. *The Journal of Neuroscience* **25**:3294-3303 https://doi.org/10.1523/jneurosci.4175-04.2005 | PubMed

Gibbs ME, Hutchinson DS, Summers RJ (2010) Noradrenaline release in the locus coeruleus modulates memory formation and consolidation; roles for α- and β-adrenergic receptors. *Neuroscience* **170**:1209-1222 https://doi.org/10.1016/j.neuroscience.2010.07.052 | PubMed

Girardeau G, Inema I, Buzsaki G. (2017) Reactivations of emotional memory in the hippocampus-amygdala system during sleep. *Nat Neurosci* **20**:1634-1642 PubMed | https://doi.org/10.1038/nn.4637

Gomperts SN, Kloosterman F, Wilson MA (2015) VTA neurons coordinate with the hippocampal reactivation of spatial experience. *eLife* **4** PubMed | https://doi.org/10.7554/eLife.05360

Groch S, Wilhelm I, Diekelmann S, Sayk F, Gais S, Born J. (2011) Contribution of norepinephrine to emotional memory consolidation during sleep. *Psychoneuroendocrinology* **36**:1342-1350 https://doi.org/10.1016/j.psyneuen.2011.03.006 | PubMed

Hagena H, Hansen N, Manahan-Vaughan D. (2016) β-Adrenergic Control of Hippocampal Function: Subserving the Choreography of Synaptic Information Storage and Memory. *Cerebral Cortex* https://doi.org/10.1093/cercor/bhv330 | PubMed

Hansen N, Manahan-Vaughan D. (2015) Locus Coeruleus Stimulation Facilitates Long-Term Depression in the Dentate Gyrus That Requires Activation of β-Adrenergic Receptors. *Cerebral Cortex* **25**:1889-1896 https://doi.org/10.1093/cercor/bht429 | PubMed

Harley CW (2007) Norepinephrine and the dentate gyrus. In: Scharfman HE (Ed). *The Dentate Gyrus: A Comprehensive Guide to Structure, Function, and Clinical Implications* **163** Progress in Brain Research Elsevier. pp. 299-318 https://doi.org/10.1016/S0079-6123(07)63018-0

Hayat H, Regev N, Matosevich N, Sales A, Paredes-Rodriguez E, Krom AJ, Bergman L, Li Y, Lavigne M, Kremer EJ, *et al.* (2020) Locus coeruleus norepinephrine activity mediates sensory-evoked awakenings from sleep. *Science Advances* **6**:eaaz4232 https://doi.org/10.1126/sciadv.aaz4232 | PubMed

Kjaerby C, Andersen M, Hauglund N, Untiet V, Dall C, Sigurdsson B, Ding F, Feng J, Li Y, Weikop P, *et al.* (2022) Memory-enhancing properties of sleep depend on the oscillatory amplitude of norepinephrine. *Nature Neuroscience* **25**:1059-1070 https://doi.org/10.1038/s41593-022-01102-9 | PubMed

Klinzing JG, Niethard N, Born J. (2019) Mechanisms of systems memory consolidation during sleep. *Nat Neurosci* **22**:1598-1610 PubMed | https://doi.org/10.1038/s41593-019-0467-3

Kuffel A, Eikelmann S, Terfehr K, Mau G, Kuehl LK, Otte C, Löwe B, Spitzer C, Wingenfeld K. (2014) Noradrenergic blockade and memory in patients with major depression and healthy participants. *Psychoneuroendocrinology* **40**:86-90 https://doi.org/10.1016/j.psyneuen.2013.11.001 | PubMed

Latchoumane CV, Ngo HV, Born J, Shin HS (2017) Thalamic Spindles Promote Memory Formation during Sleep through Triple Phase-Locking of Cortical, Thalamic, and Hippocampal Rhythms. *Neuron* **95**:424-435 e6 PubMed | https://doi.org/10.1016/j.neuron.2017.06.025

Logothetis NK (2015) Neural-Event-Triggered fMRI of large-scale neural networks. *Curr Opin Neurobiol* **31**:214-22 PubMed | https://doi.org/10.1016/j.conb.2014.11.009

Logothetis NK, Eschenko O, Murayama Y, Augath M, Steudel T, Evrard HC, Besserve M, Oeltermann A. (2012) Hippocampal-cortical interaction during periods of subcortical silence. *Nature* **491**:547-53 PubMed | https://doi.org/10.1038/nature11618

Maingret N, Girardeau G, Todorova R, Goutierre M, Zugaro M. (2016) Hippocampo-cortical coupling mediates memory consolidation during sleep. *Nat Neurosci* **19**:959-964 https://doi.org/10.1038/nn.4304 | PubMed

Miranda MI, Ortiz-Godina F, García D. (2009) Differential involvement of cholinergic and beta-adrenergic systems during acquisition, consolidation, and retrieval of long-term memory of social and neutral odors. *Behavioural Brain Research* **202**:19-25 https://doi.org/10.1016/j.bbr.2009.03.008 | PubMed

Molle M, Yeshenko O, Marshall L, Sara SJ, Born J. (2006) Hippocampal sharp wave-ripples linked to slow oscillations in rat slow-wave sleep. *J Neurophysiol* **96**:62-70 PubMed | https://doi.org/10.1152/jn.00014.2006

Nitzan N, Swanson R, Schmitz D, Buzsáki G. (2022) Brain-wide interactions during hippocampal sharp wave ripples. *Proc Natl Acad Sci U S A* **119**:e2200931119 https://doi.org/10.1073/pnas.2200931119 | PubMed

Norimoto H, Makino K, Gao M, Shikano Y, Okamoto K, Ishikawa T, Sasaki T, Hioki H, Fujisawa S, Ikegaya Y. (2018) Hippocampal ripples down-regulate synapses. *Science* **359**:1524-1527 https://doi.org/10.1126/science.aao0702 | PubMed

Novitskaya Y, Sara SJ, Logothetis NK, Eschenko O. (2016) Ripple-triggered stimulation of the locus coeruleus during post-learning sleep disrupts ripple/spindle coupling and impairs memory consolidation. *Learn Mem* **23**:238-48 PubMed | https://doi.org/10.1101/lm.040923.115

Osorio-Forero A, Cardis R, Vantomme G, Guillaume-Gentil A, Katsioudi G, Devenoges C, Fernandez LMJ, Lüthi A. (2021) Noradrenergic circuit control of non-REM sleep substates. *Current Biology* **31**:5009-5023.e7. https://doi.org/10.1016/j.cub.2021.09.041 | PubMed

Palacios-Filardo J, Mellor JR (2019) Neuromodulation of hippocampal long-term synaptic plasticity. *Current Opinion in Neurobiology* **54**:37-43 https://doi.org/10.1016/j.conb.2018.08.009 | PubMed

Paxinos G, Watson C. (2005) *The rat brain in stereotaxic coordinates* (5th) Amsterdam; Boston: Elsevier Academic Press.

Peyrache A, Battaglia FP, Destexhe A. (2011) Inhibition recruitment in prefrontal cortex during sleep spindles and gating of hippocampal inputs. *Proceedings of the National Academy of Sciences* **108**:17207-17212 https://doi.org/10.1073/pnas.1103612108 | PubMed

Poe GR (2017) Sleep Is for Forgetting. *The Journal of Neuroscience* **37**:464-473 https://doi.org/10.1523/jneurosci.0820-16.2017 | PubMed

Przybyslawski J, Roullet P, Sara SJ (1999) Attenuation of emotional and nonemotional memories after their reactivation: role of beta adrenergic receptors. *J Neurosci* **19**:6623-8 https://doi.org/10.1523/jneurosci.19-15-06623.1999 | PubMed

Roullet P, Sara S. (1998) Consolidation of memory after its reactivation: involvement of beta noradrenergic receptors in the late phase. *Neural Plast* **6**:63-8 https://doi.org/10.1155/np.1998.63 | PubMed

Sadowski JLP, Jones M, Mellor J. (2016) Sharp-Wave Ripples Orchestrate the Induction of Synaptic Plasticity during Reactivation of Place Cell Firing Patterns in the Hippocampus. *Cell Reports* **14**:1916-1929 https://doi.org/10.1016/j.celrep.2016.01.061 | PubMed

Sara SJ (2009) The locus coeruleus and noradrenergic modulation of cognition. *Nat Rev Neurosci* **10**:211-23 https://doi.org/10.1038/nrn2573 | PubMed

Sara SJ, Roullet P, Przybyslawski J. (1999) Consolidation of memory for odor-reward association: beta-adrenergic receptor involvement in the late phase. *Learn Mem* **6**:88-96 https://doi.org/10.1101/lm.6.2.88 | PubMed

Sara SJ (2017) Sleep to Remember. *The Journal of Neuroscience* **37**:457-463 https://doi.org/10.1523/JNEUROSCI.0297-16.2017 | PubMed

Sara SJ, Bouret S. (2012) Orienting and reorienting: the locus coeruleus mediates cognition through arousal. *Neuron* **76**:130-141 https://doi.org/10.1016/j.neuron.2012.09.011 | PubMed

Selinger JV, Kulagina NV, O'Shaughnessy TJ, Ma W, Pancrazio JJ (2007) Methods for characterizing interspike intervals and identifying bursts in neuronal activity. *J Neurosci Methods* **162**:64-71 PubMed | https://doi.org/10.1016/j.jneumeth.2006.12.003

Skelin I, Kilianski S, McNaughton BL (2018) Hippocampal coupling with cortical and subcortical structures in the context of memory consolidation. *Neurobiology of Learning and Memory* https://doi.org/10.1016/j.nlm.2018.04.004 | PubMed

Straube T, Frey JU (2003) Involvement of beta-adrenergic receptors in protein synthesis-dependent late long-term potentiation (LTP) in the dentate gyrus of freely moving rats: the critical role of the LTP induction strength. *Neuroscience* **119**:473-9 PubMed | https://doi.org/10.1016/s0306-4522(03)00151-9

Swift KM, Gross BA, Frazer MA, Bauer DS, Clark KJD, Vazey EM, Aston-Jones G, Li Y, Pickering AE, Sara SJ, *et al.* (2018) Abnormal locus coeruleus sleep activity alters sleep signatures of memory consolidation and impairs place cell stability and spatial memory. *Current Biology* **28**:3599-3609.e4. https://doi.org/10.1016/j.cub.2018.09.054 | PubMed

Takahashi K, Kayama Y, Lin JS, Sakai K. (2010) Locus coeruleus neuronal activity during the sleep-waking cycle in mice. *Neuroscience* **169**:1115-26 PubMed

Tang W, Shin JD, Frank LM, Jadhav SP (2017) Hippocampal-Prefrontal Reactivation during Learning Is Stronger in Awake Compared with Sleep States. *The Journal of Neuroscience* **37**:11789-11805 https://doi.org/10.1523/jneurosci.2291-17.2017 | PubMed

Totah NK, Neves RM, Panzeri S, Logothetis NK, Eschenko O. (2018) The Locus Coeruleus Is a Complex and Differentiated Neuromodulatory System. *Neuron* **99**:1055-1068 e6 PubMed | https://doi.org/10.1016/j.neuron.2018.07.037

Ul Haq R, Liotta A, Kovacs R, Rösler A, Jarosch MJ, Heinemann U, Behrens CJ (2012) Adrenergic modulation of sharp wave-ripple activity in rat hippocampal slices. *Hippocampus* **22**:516-533 https://doi.org/10.1002/hipo.20918 | PubMed

Varela F, Lachaux JP, Rodriguez E, Martinerie J. (2001) The brainweb: Phase synchronization and large-scale integration. *Nature Reviews Neuroscience* **2**:229-239 https://doi.org/10.1038/35067550 | PubMed

Vazey EM, Aston-Jones G. (2014) Designer receptor manipulations reveal a role of the locus coeruleus noradrenergic system in isoflurane general anesthesia. *Proceedings of the National Academy of Sciences of the United States of America* **111**:3859-3864 https://doi.org/10.1073/pnas.1310025111 | PubMed

Wang DV, Ikemoto S. (2016) Coordinated Interaction between Hippocampal Sharp-Wave Ripples and Anterior Cingulate Unit Activity. *The Journal of Neuroscience* **36**:10663-10672 https://doi.org/10.1523/jneurosci.1042-16.2016 | PubMed

Wang DV, Yau HJ, Broker CJ, Tsou JH, Bonci A, Ikemoto S. (2015) Mesopontine median raphe regulates hippocampal ripple oscillation and memory consolidation. *Nat Neurosci* https://doi.org/10.1038/nn.3998 | PubMed

Yang M, Logothetis NK, Eschenko O. (2019) Occurrence of Hippocampal Ripples is Associated with Activity Suppression in the Mediodorsal Thalamic Nucleus. *J Neurosci* **39**:434-444 PubMed | https://doi.org/10.1523/JNEUROSCI.2107-18.2018

Peer reviews

Reviewer #1 (Public review):

Summary:

The manuscript by Yang et al. investigates the relationship between multi-unit activity in the locus coeruleus, putatively noradrenergic locus coeruleus, hippocampus (HP) sharp-wave ripples (SWR) and spindles using multi-site electrophysiology in freely behaving male rats. The study focuses on SWR during quiet wake and non-REM sleep, and their relation to cortical states (identified using EEG recordings in frontal areas) and LC units.

The manuscript highlights differential modulation of LC units as a function of HP-cortical communication during wake and sleep. They establish that ripples and LC units are inversely correlated to levels of arousal: wake, i.e. higher arousal correlates with higher LC unit activity and lower ripple rates. The authors show that LC neuron activity is strongly inhibited just before SWR detected during wake. During non-REM sleep, they distinguish "isolated" ripples from SWR coupled to spindles and show that inhibition of LC neuron activity is absent before spindle-coupled ripples but not before isolated ripples, suggesting a mechanism where noradrenaline (NA) tone is modulated by HP-cortical coupling. This result has interesting implications for the roles of noradrenaline in the modulation of sleep-dependent memory consolidation, as ripple-spindle coupling is a mechanism favoring consolidation. The authors further show that NA neuronal activity is downregulated before spindles.

Strengths:

In continuity with previous work from the laboratory, this work expands our understanding of the activity of neuromodulatory systems in relation to vigilance states and brain oscillations, an area of research that is timely and impactful. The manuscript presents strong results suggesting that NA tone varies differentially depending on coupling of HP SWR with cortical spindles. The authors place their findings back in the context of identified roles of HP ripples and coupling to cortical oscillations for memory formation in a very interesting discussion. The distinction of LC neuron activity between awake, ripple-spindle coupled events and isolated ripples is an exciting result and its relation to arousal and memory opens fascinating lines of research.

Weaknesses:

I regretted that the paper fell short of trying to push this line of idea a bit further, for example by contrasting in the same rats the LC unit-HP ripple coupling during exploration of a highly familiar context (as seemingly was the case in their study) versus a novel context, which would increase arousal and trigger memory-related mechanisms. Any kind of manipulation of arousal levels and investigation of the impact on awake vs nonREM sleep LC-HP ripple coordination would considerably strengthen the scope of the study.

Comments on revised version.

The authors have added methodological details to the results section after the first round of reviews, improving the manuscript readability. Some points might still be improved, for example, the authors use a delta/gamma ratio to track cortical states for example, but there is no methods section corresponding to this metric. Authors write that higher SI corresponds to a lower arousal state that is associated with "more synchronized cortical population activity, higher ripple rate and reduced LC neurons firing" but there are no references or analysis to support this statement, only examples showing changes in SI over a few minutes.

https://doi.org/10.7554/eLife.109159.2.sa3

Reviewer #2 (Public review):

Summary:

In this study, authors studied the synchrony between ripple events in Hippocampus, cortical spindles and Locus Coeruleus spiking. The results in this study together with the established literature on the relationship of hippocampal ripples with widespread thalamic and cortical waves, guided authors to propose a role for Locus Coeruleus spiking patterns in memory consolidation. The findings provided here, i.e. correlations between LC spiking activity and Hippocampal ripples, could provide basis for future studies probing the directional flow or the necessity of these correlations in the memory consolidation process. Hence, the paper provides enough scientific advance to highlight the elusive yet important role of Norepinephrine circuitry in the memory processes.

Strengths:

Authors were able to demonstrate correlations of Locus Coeruleus spikes with hippocampal ripples as well as with cortical spindles. Specific strength of the paper is in the demonstration that the spindles that activate with the ripples are comparatively different in their correlations with Locus Coeruleus than those which do not.

Weaknesses:

The claims regarding the roles of these specific interactions were mostly derived from the literature that these processes individually contribute to the memory process, without any evidence of these specific interactions being necessary for memory processes. There are also issues with the description of methods, validation of shuffling procedures and unclear presentation and the interpretation of the findings, which are described in points that follow. I believe addressing these weaknesses might improve and add to the strength of the findings.

Comments on revised version.

The authors addressed all of my major concerns during the revision. As a result, the study now provides convincing evidence as well as improved presentation of results, that makes this manuscript important to the broader field of neuroscience, beyond the specific sub-field.

https://doi.org/10.7554/eLife.109159.2.sa2

Reviewer #3 (Public review):

This manuscript examines how locus coeruleus (LC) activity relates to hippocampal ripple events across behavioral states in freely moving rats. Using multi-site electrophysiological recordings, the authors report that LC activity is suppressed prior to ripple events, with the magnitude of suppression depending on ripple subtype. Suppression is stronger during wakefulness than during NREM sleep and least pronounced for ripples coupled to spindles.

The study is technically sound and addresses a timely and important question regarding how LC activity interacts with hippocampal and thalamocortical network events across vigilance states. While the findings are interesting, they remain observational in nature. Following revision, the manuscript has substantially improved in both presentation and interpretation of the results, and most concerns have been addressed satisfactorily. I therefore only have a few minor considerations that the authors may wish to explore further in the current study or in future work, as these directions could provide additional mechanistic insight and would likely be of considerable interest to the field.

The authors demonstrate clearly that tonic LC firing rates preceding ripples differ significantly between wake-associated ripples (highest LC firing), isolated ripples during NREM sleep (lower LC firing), and spindle-coupled ripples (lowest LC firing). They also appropriately note that baseline firing differences will naturally influence the magnitude of LC suppression, which they also observe (highest LC reduction for wake ripples, then isolated ripples and last spindle-coupled ripples). However, this aspect could be explored further, as it may provide additional insight into the regulation of spindle-associated ripple events. Since LC activity appears to decline gradually prior to ripple occurrence (Suppl. Figure 2), it would be interesting to test whether this gradual reduction helps organize the emergence of isolated versus spindle-coupled ripples. For example, isolated ripples may occur during the initial phase of LC decline, whereas spindle-coupled ripples may preferentially emerge when LC activity reaches its lowest levels. Such a relationship could also be consistent with the stronger synchronization observed for spindle-ripple coupling.

Related to this point, it would also be informative to examine whether isolated spindles occur more randomly in time, whereas spindle-associated ripple events appear more temporally clustered. If a single isolated spindle occurs, the associated LC suppression might be more pronounced. In contrast, when multiple spindle-associated ripple events occur in succession, LC activity may already be reduced following the first event, resulting in smaller additional suppression preceding subsequent events. Exploring this possibility could help clarify how LC dynamics shape the temporal emergence of ripple-subtypes

https://doi.org/10.7554/eLife.109159.2.sa1

Author response:

The following is the authors' response to the original reviews.

> ***Reviewer #1 (Public review):***
>
> *Summary:*
>
> *The manuscript by Yang et al. investigates the relationship between multi-unit activity in the locus coeruleus, putatively noradrenergic locus coeruleus, hippocampus (HP), sharp-wave ripples (SWR), and spindles using multi-site electrophysiology in freely behaving male rats. The study focuses on SWR during quiet wake and non-REM sleep, and their relation to cortical states (identified using EEG recordings in frontal areas) and LC units.*
>
> *The manuscript highlights differential modulation of LC units as a function of HP-cortical communication during wake and sleep. They establish that ripples and LC units are inversely correlated to levels of arousal: wake, i.e., higher arousal correlates with higher LC unit activity and lower ripple rates. The authors show that LC neuron activity is strongly inhibited just before SWR is detected during wake. During non-REM sleep, they distinguish "isolated" ripples from SWR coupled to spindles and show that inhibition of LC neuron activity is absent before spindle-coupled ripples but not before isolated ripples, suggesting a mechanism where noradrenaline (NA) tone is modulated by HP-cortical coupling. This result has interesting implications for the roles of noradrenaline in the modulation of sleep-dependent memory consolidation, as ripple-spindle coupling is a mechanism favoring consolidation. The authors further show that NA neuronal activity is downregulated before spindles.*
>
> *Strengths:*
>
> *In continuity with previous work from the laboratory, this work expands our understanding of the activity of neuromodulatory systems in relation to vigilance states and brain oscillations, an area of research that is timely and impactful. The manuscript*

> *presents strong results suggesting that NA tone varies differentially depending on the coupling of HP SWR with cortical spindles. The authors place their findings back in the context of identified roles of HP ripples and coupling to cortical oscillations for memory formation in a very interesting discussion. The distinction of LC neuron activity between awake, ripple-spindle coupled events and isolated ripples is an exciting result, and its relation to arousal and memory opens fascinating lines of research.*
>
> *Weaknesses:*
>
> *I regretted that the paper fell short of trying to push this line of idea a bit further, for example, by contrasting in the same rats the LC unit-HP ripple coupling during exploration of a highly familiar context (as seemingly was the case in their study) versus a novel context, which would increase arousal and trigger memory-related mechanisms. Any kind of manipulation of arousal levels and investigation of the impact on awake vs non-REM sleep LC-HP ripple coordination would considerably strengthen the scope of the study.*

We agree that conducting specific behavioral tests before electrophysiological recordings, as well as manipulating arousal during the recording session, would strengthen the study. These experiments are planned for future work, and we acknowledged this point in the discussion.

We added the following text in the Discussion: “Conducting behavioral assays prior to electrophysiological recordings, along with spatially and temporally precise modulation of LC activity during recording sessions, will be essential for achieving a mechanistic understanding of network dynamics and its functional role for memory consolidation in future investigations.”

> *The main result shows that LC units are not modulated during non-REM sleep around spindle-coupled ripples (named spRipples, 17.2% of detected ripples); they also show that LC units are modulated around ripple-coupled spindles (ripSpindles, proportion of detected spindles not specified, please add). These results seem in contradiction; this point should be addressed by the authors.*

The detection of coupled events - spindle-coupled ripples (spRipple) and ripple-coupled spindles (ripSpindle) - was performed independently, although, some overlap cannot be excluded. We found that LC suppression was generally weak around both types of coupled events. Specifically, LC suppression around spRipples and ripSpindles reached significance (exceeding the 95% confidence interval) in 4 sessions (from 3 rats) and 3 sessions (from 2 rats), respectively, out of a total of 20 sessions (from 7 rats).

We revised the manuscript by providing additional information in the Results section and adding a Supplementary Figure 5 showing a significant correlation (Pearson r = 0.72, p = 0.0003) between the modulation index (MI) for spRipple and ripSpindle.

> *Results are displayed per recording session, with 20 sessions total recorded from 7 rats (2 to 8 sessions per rat), which implies that one of the rats accounts for 40% of the dataset. Authors should provide controls and/or data displayed as average per rat to ensure that results are now skewed by the weight of that single rat in the results.*

High-quality recordings from the LC in behaving rats are technically challenging and relatively rare; therefore, we included all valid datasets in analysis. The average modulation index (MI), calculated per animal and per session, fell within a consistent range (Supplementary Figure 3) despite variability in the number of recording sessions (2–8 sessions per rat).

> *In its current form, the manuscript presents a lack of methodological detail that needs to be addressed, as it clouds the understanding of the analysis and conclusions. For*

> *example, the method to account for the influence of cortical state on LC MUA is unclear, both for the exact methods (shuffling of the ripple or spindle onset times) and how this minimizes the influence of cortical states; this should be better described. If the authors wish to analyze unit modulation as a function of cortical state, could they also identify/sort based on cortical states and then look at unit modulation around ripple onset? For the first part of the paper, was an analysis performed on quiet wake, non-REM sleep, or both?*

The LC activity around rippled was modulated at multiple temporal scales. First, we observed a relatively sharp drop in the LC firing rate ~ 2 s before the ripple onset. When computing peri-ripple LC activity over a longer time window ([–12, 12] sec), we observed a rather slow decrease in the LC firing rate beginning as early as 10 s before the ripple onset (Supplementary Figure 2).

Considering two temporal scales, we hypothesized that slow modulation of LC activity might be related to fluctuations of the global brain state. We quantified the ongoing cortical state using a synchronization index (SI), calculated as a power ratio (1–4 Hz/30–90 Hz) of the EEG within 4-s windows and computed the corresponding ripple and LC-MUA rates. Figure 3A (in the main manuscript) illustrates that a higher SI (more synchronized cortical population activity) corresponded to a lower arousal state and reduced LC tonic firing; this brain state was associated with a higher ripple activity. As shown in the new Figure 3B, the LC firing rate was negatively correlated with the SI and ripple rate. Thus, slow LC modulation was likely driven by cortical state transitions.

To correct for the influence of the global brain state on the peri-ripple LC activity, we generated surrogate events by jittering the times of detected ripples. First, we confirmed that triggering the hippocampal LFP on the surrogate events lacked the ripple-specific frequency component (main Figure 3C) and the SI state did not differ around ripples and surrogate events (main Figure 3D). Plotting the LC activity around surrogate evens captured its state-dependent dynamics (Figure 3 or Supplementary Figure 2, orange trace). To extract state-independent peri-ripple LC modulation, we subtracted the state-related LC activity (orange trace) from the ripple-triggered LC activity (blue trace). The resulting trace yielded a corrected estimate of ripple-associated LC activity that was largely free from the confounding influence of cortical state transitions (main Figure 3E).

In the Results subsection “LC-NE neuron spiking is suppressed around hippocampal ripples”, we reported LC modulation without accounting for the cortical state (main Figure 2). The state-dependent effects were instead examined in the subsequent Results subsection, “LC firing and ripple occurrence are state-dependent and inversely related” we report state-corrected LC modulation (main Figure 3). Finally, in the Results subsection “Peri-ripple LC modulation depends on the cortical–hippocampal interaction,” we characterized LC activity around ripples across different cortical states (quite awake and NREM sleep).

We revised Methods and Results to provide more methodological details and a rationale for each analysis, as requested.

> ***Reviewer #2 (Public review):***
>
> *Summary:*
>
> *In this study, the authors studied the synchrony between ripple events in the Hippocampus, cortical spindles, and Locus Coeruleus spiking. The results in this study, together with the established literature on the relationship of hippocampal ripples with widespread thalamic and cortical waves, guided the authors to propose a role for Locus Coeruleus spiking patterns in memory consolidation. The findings provided here, i.e., correlations between LC spiking activity and Hippocampal ripples, could provide a basis*

> *for future studies probing the directional flow or the necessity of these correlations in the memory consolidation process. Hence, the paper provides enough scientific advances to highlight the elusive yet important role of Norepinephrine circuitry in the memory processes.*
>
> *Strengths:*
>
> *The authors were able to demonstrate correlations of Locus Coeruleus spikes with hippocampal ripples as well as with cortical spindles. A specific strength of the paper is in the demonstration that the spindles that activate with the ripples are comparatively different in their correlations with Locus Coeruleus than those that do not.*
>
> *Weaknesses:*
>
> *The claims regarding the roles of these specific interactions were mostly derived from the literature that these processes individually contribute to the memory process, without any evidence of these specific interactions being necessary for memory processes. There are also issues with the description of methods, validation of shuffling procedures, and unclear presentation and the interpretation of the findings, which are described in the points that follow. I believe addressing these weaknesses might improve and add to the strength of the findings.*

We believe that our responses to the Reviewer 1 and Reviewer 2, corresponding revisions of the manuscript and new figures adequately addressed all issues raised by the Reviewer 2.

> ***Reviewer #3 (Public review):***
>
> *Summary:*
>
> *This manuscript examines how locus coeruleus (LC) activity relates to hippocampal ripple events across behavioral states in freely moving rats. Using multi-site electrophysiological recordings, the authors report that LC activity is suppressed prior to ripple events, with the magnitude of suppression depending on the ripple subtype. Suppression is stronger during wakefulness than during NREM sleep and is least pronounced for ripples coupled to spindles.*
>
> *The study is technically competent and addresses an important question regarding how LC activity interacts with hippocampal and thalamocortical network events across vigilance states.*
>
> *Weaknesses:*
>
> *The results are interesting, but entirely observational. Also, the study in its current form would benefit from optimization of figure labeling and presentation, and more detailed result descriptions to make the findings fully interpretable. Also, it would be beneficial if the authors could formulate the narrative and central hypothesis more clearly to ease the line of reasoning across sections.*

We improved the presentation of results by incorporating additional figures and expanding the detail in the figure captions. In the main text, we clarified specific hypotheses and provided a rationale underlying each analysis.

> *Comments:*
>
> *(1) Stronger evidence that recorded units represent noradrenergic LC neurons would reinforce the conclusions. While direct validation may not be possible, showing absolute firing rates (Hz) across quiet wake, active wake, NREM, and REM, and comparing them to published LC values, would help.*

We added the requested data and a Supplementary Figure 1 in the revised manuscript: “The average firing rates of LC single units were 1.70 ± 0.21 Hz during wakefulness, 0.51 ± 0.07 Hz during NREM sleep, and 0.014 ± 0.01 Hz during REM sleep (Supplementary Figure 1). Firing rates differed significantly across arousal states, with the highest activity during wakefulness, reduced activity during NREM sleep, and minimal activity during REM sleep (one-way ANOVA: $F(2,38) = 39.8$, $p < 0.0001$). This firing pattern is characteristic of LC-NE neurons and is consistent with existing literature.”

> *(2) The analyses rely almost exclusively on z-scored LC firing and short baselines (~4-6 s), which limits biological interpretation. The authors should include absolute firing rates alongside normalized values for peri-ripple and peri-spindle analyses and extend pre-event windows to at least 20-30 s to assess tonic firing evolution. This would clarify whether differences across ripple subtypes arise from ceiling or floor effects in LC activity; if ripples require LC silence, the relative drop will appear larger during high-firing wake states. This limitation should be discussed and, if possible, results should be shown based on unnormalized firing rates.*

We agree with the reviewer that a longer pre-event window provides a clearer estimate of baseline LC activity. However, given that both ripples and spindles are brief oscillatory events, we tested a range of time windows and found that a 12-s interval adequately captures baseline LC activity dynamics. Accordingly, we included plots with extended pre-event windows (−12 to 12 s), as requested.

We added in the revised manuscript absolute firing rates for well-isolated LC single units. Because the number of neurons contributing to LC multi-unit activity (LC-MUA) is unknown, we avoided averaging absolute firing rates for this signal. For LC-MUA, we implemented a normalization approach in which firing rates (50-ms bins) around ripple or spindle are scaled to a baseline period preceding the trigger event (−12 to −10 s). Importantly, unlike z-scoring, this normalization method preserves baseline differences across behavioral states. As shown in Author response image 1A and new Figure 5 in the main manuscript, baseline LC firing rates were highest prior to awake ripples and lowest prior to sleep spindles. During ripples occurring in wakefulness, LC activity did not decrease to the levels observed during sleep. In contrast, during NREM sleep, LC activity was downregulated during both ripples and spindles, although it did not reach complete silence around either oscillatory event.

Author response image 1B illustrates a slow downward drift in the LC firing rate preceding either ripple or spindle. The slow LC dynamics likely reflected gradual transitions toward more synchronized brain state, which is optimal for ripple generation. In contrast, event-specific LC modulation had faster dynamics (Author response image 1B, highlighted interval) and was largely absent in cases where spRipples and ripSpindles were not associated with LC suppression (Author response image 1C).

To minimize the influence of global state fluctuations and emphasize event-related dynamics, we therefore presented the main results using state-corrected and z-scored PETHs.

Please also refer to our response to Reviewer 1 regarding the two temporal scales of LC modulation.

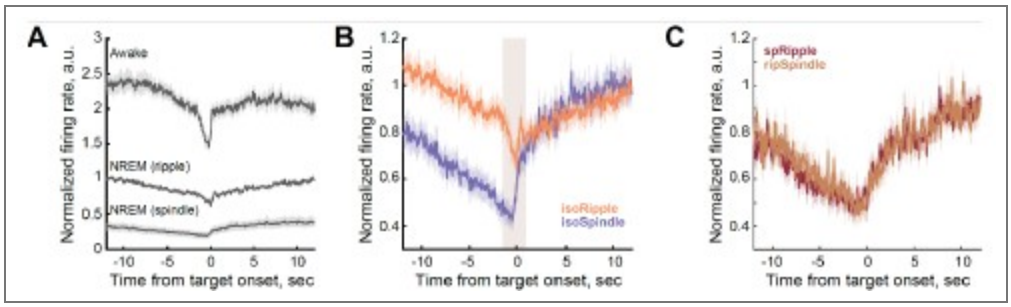

Author response image 1. LC modulation around sleep oscillations. (A) Peri-event LC-MUA during awake and NREM sleep. LC activity and the range of peri-event LC modulation differed across behavioral states; it was overall higher preceding ripples occurring in wakefulness than in NREM sleep, and it was the lowest around sleep spindles. Despite the state-dependent differences in the firing rate, LC modulation was observed around all oscillatory events. During wakefulness, LC activity did not decrease to the levels observed during NREM sleep. During NREM sleep, LC activity was down-regulated around both ripples and spindles, and the LC firing did not completely cease around either oscillatory event. (B) Peri-event LC-MUA around isolated oscillatory events. LC activity exhibited fast peri-event dynamics (highlighted interval) superimposed on slower, state-dependent fluctuations. (C) Peri-event LC-MUA around coupled oscillatory events. Fast peri-event LC modulation was absent, while slow fluctuations were preserved around coupled oscillatory events. For all plots, LC-MUA firing rate was scaled to a pre-event baseline interval [-12 to -10 sec] to preserve baseline differences in LC activity across behavioral states. Bin size: 50 ms. isoRipple – isolated ripple, isoSpindle – isolated spindle, spRipple - spindle-coupled ripple, ripSpindle - ripple-coupled spindle.}

> *(3) Because spindles often occur in clusters, the timing of ripple occurrence within these clusters could influence LC suppression. Indicate whether this structure was considered or discuss how it might affect interpretation (e.g., first vs. subsequent ripples within a spindle cluster).*

We did not consider spindle clusters and classified the event as ripple-coupled spindle if the ripple occurred between the spindle on and offset.

> *(4) While the observational approach is appropriate here, causal tests (e.g., optogenetic or chemogenetic manipulation of LC around ripple events and in memory tasks) would considerably strengthen the mechanistic conclusions. At a minimum, a discussion of how such approaches could address current open questions would improve the manuscript.*

We agree that conducting causal tests would strengthen the study. We added the following text in the Discussion: “Conducting behavioral assays prior to electrophysiological recordings, along with spatially and temporally precise modulation of LC activity during recording sessions, will be essential for achieving a mechanistic understanding of network dynamics and its functional role for memory consolidation in future investigations.”

> *(5) Please show how "Synchronization Index" (SI) differs quantitatively across behavioral states (wake, NREM, REM) and discuss whether it could serve as a state classifier. This would strengthen interpretations of the correlations between SI, ripple occurrence, and LC activity.*

We plotted the awake state-normalized SIs for awake and NREM sleep. Due to small number of REM sleep episodes, SI for REM sleep is not shown. The average SI during NREM sleep was significantly higher than during awake state, consistent with the well-established dominance of low-frequency (1-4 Hz) oscillatory power and reduced high-frequency (30-90 Hz) power during NREM sleep.

Although SI could potentially serve as a behavioral state classifier, we have chosen not to address this point to maintain the focus in the discussion on new results.

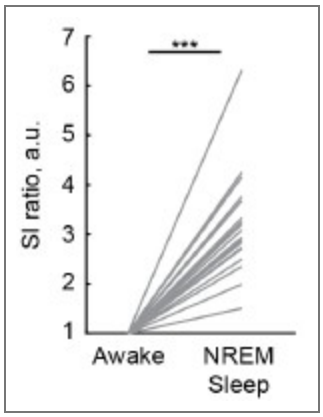

Author response image 2. **Synchronization index differentiates behavioral states.**

> *(6) The current use of SI to denote a delta/gamma power ratio is unconventional, as "SI" typically refers to phase-locking metrics. Consider adopting a more standard term, such as delta/gamma power ratio. Similarly, it would be easier to follow if you use common terminology (AUC) to describe the drop in LC-MUA rather than using "MI" and "sub-MI".*

The ranges of delta and gamma bands might vary across studies; therefore, we prefer using SI, as defined here and in our previous publications (Novitskaya et al., 2016; Yang et al., 2019, 2021). We calculated the modulation index (MI) as the area under the curve of the peri-event time histogram within the 1 second preceding ripple onset. To avoid potential confusion with the AUC calculated over the entire signal window, we opted to use MI.

> *(7) The logic in Figure 3 is difficult to follow. The brain state (delta/gamma ratio) appears unchanged relative to surrogate events (3C), while LC activity that is supposedly negatively correlated to delta/gamma changes markedly (3D-E). Could this discrepancy reflect the low temporal resolution (4-s windows) used to calculate delta/gamma when the changes occur on a shorter time scale?*

We appreciate the reviewer's question. We revised the results and Figure 3 legend to clarify this point. The main Figures 3E and 3F show the 'state-corrected' peri-ripple LC activity. The purpose of generating 'surrogate' events was precisely to capture the component of LC activity dynamics that can be explained by cortical state fluctuations alone. As shown in Supplementary Figure 2, the orange trace represents LC activity aligned to surrogate events and, as the Reviewer noted, shows a clear decrease, yet at a slower time scale. We interpret this surrogate-aligned signal as the LC modulation attributable specifically to cortical state fluctuations. Importantly, shuffled events were associated with similar SIs (cortical state), but absent HPC LFP power increase in the ripple range (140-250 Hz), as shown in the main Figures 3C and 3D, respectively. To isolate the peri-event LC dynamics, we subtracted the state-related component (Figure 3, orange trace) from the ripple-triggered LC activity (blue trace). This correction yielded an estimate of ripple-associated LC activity that is largely independent of the confounding influence of ongoing cortical state.

Please, see our detailed response to the Reviewer 1 about multiple time scales of LC dynamics.

> *(8) There are apparent inconsistencies between Figures 4B and 4C-D. In B, it seems that the difference between the 10th and 90th percentile is mostly in higher frequencies, but in C and D, the only significant difference is in the delta band.*

We repeated this analysis, clarified inconsistency, and revised Figure 4 legend.

> *(9) Because standard sleep scoring is based on EEG and EMG signals, please include an example of sleep scoring alongside the data used for state classification. It would also be relevant to include the delta/gamma power ratio in such an example plot.*

We replaced 'standard' with 'previously established" sleep scoring procedure and added a Supplementary Figure 4 showing representative NREM sleep and wake episodes with corresponding EEG and SI.

> *(10) Can variability in modulation index (subMI) across ripple subsets reflect differences in recording quality? Please report and compare mean LC firing rates across subsets to confirm this is not a confounding factor.*

We agree that considering recording quality and unit stability over time as potential confounding factors is important. We therefore carefully evaluated each dataset to ensure the absence of significant drift in the LC firing rate. However, we find that comparing mean LC firing rates across subsets of ripples, as suggested by the Reviewer, is insufficient to control for recording stability, as LC activity varies substantially across behavioral states. At present, we are not aware of a robust method to fully eliminate variability related to recording quality and unit stability over time.

> *(11) Figure 6B: If the brown trace represents LC-MUA activity around random time points, why would there be a coinciding negative peak as relative to real sleep spindles? Or is it the subtracted trace?*

We have revised Figure 7 (original Figure 6) and its legend to improve clarity and readability.

> *(12) On page 8, lines 207-209, the authors write "Importantly, neither the LC-MUA rate nor SIs differed during a 2-sec time window preceding either group of spindles". It is unclear which data they refer to, but the statement seems to contradict Figure 6E as well as the following sentence: "Across sessions, MI values exceeded 95% CI in 17/20 datasets for isoSpindles and only 3/20 for ripSpindles". This should be clarified.*

We have revised the corresponding text to improve clarity and readability.

> *(13) The results in Figures 5C and 6F do not align. It seems surprising that ripple-coupled spindles show a considerably higher LC modulation than spindle-coupled ripples, as these events should overlap. Could the discrepancy be due to Z-score normalization as mentioned above? Please include a discussion of this to help the interpretation of the results.*

In the original manuscript, Figure 6F was mistakenly labelled for ripple-coupled (ripSpindles) and isolated (isoSpindles) spindles. Now it has been corrected.

Please, also see our response to the Reviewer 1 weaknesses.

> *(14) The text implies that 8 recordings came from one rat and two each from six others. This should be confirmed, and it should be explained how the recordings were balanced and analyzed across animals.*

Since high-quality recordings from LC in behaving animals are challenging and rare, we used all valid sessions. We addressed the same point in our response to the Reviewer 1 weaknesses.

> ***Recommendations for the authors:***
>
> ***Reviewer #1 (Recommendations for the authors):***

> *Below are some suggestions for clarification/information that are needed to improve the paper's readability (and the understanding of the analysis and methods).*
>
> *(1) The authors describe a consistently negative correlation between cortical EEG synchronization index and ripple rate or LC-MUA, show an example in Figure 3A, and report a range of r values in the text with a mention of p < 0.01. The reported p-value is presumably the highest p-value for the correlations - please specify. Visualization of the results might be improved by adding example correlations (also true for later correlations in Figure 6).*

We revised the result description accordingly and included correlation plots in Figures 3 and 7.

> *(2) Description of statistical testing is missing for Figure 3C (nothing in the text or the figure legend); there is also no statistics section in the methods. For Figure 4, the statistics are reported for the Friedman test but not the post-hoc tests. Exact p-value and statistics should be reported for the comparison of LC-MUA rate and SI in the 2 s preceding spindles.*

We have added the statistical results requested and revised figure legends by providing additional information. We added the Statistic Analysis section in the Methods.

Figure 3D (original Fig.3C): “Average Synchronization Index (SI) around ripples and shuffled events. The cortical state preceding shuffled events and ripples was comparable, as confirmed by the absence of significant differences in SI (Wilcoxon signed-rank test; shuffled: Z = -0.20, p = 0.84; ripples: Z = 0.14, p = 0.88). Cortical synchrony increased following both events (shuffled: Z = -3.50, p = 0.00044; ripples: Z = -3.66, p = 0.00026). Similar cortical state dynamics surrounding shuffled events and ripples indicate that the surrogate events adequately capture the cortical state associated with ripple occurrence.

Figure 6: Intra-ripple frequency (A) and peak amplitude (B) for different ripple types. Boxwhisker plots show the median, the 1st and 3rd quartiles, and min/max. Gray dots show data from individual rats. *** - p < 0.001 for post hoc pairwise comparisons (Wilcoxon signed-rank tests with Holm–Bonferroni correction for multiple comparisons).

We revised the Results accordingly: “The ripple subtypes differed in the intra-ripple frequency (Friedman test, chi2 = 35.62, p < 0.0001, post hoc pairwise comparisons were performed using Wilcoxon signed-rank tests with Holm–Bonferroni correction for multiple comparisons. awRipple vs isoRipple: p = 0.00003 awRipple vs spRipple: p = 0.00004 isoRipple vs spRipple: p = 0.0002}), with awRipples being the fastest and spRipples the slowest (Figure 6A).There was no difference in the ripple peak amplitude (Friedman test, χ2 = 3.7, p = 0.16; Figure 6B).”

> *(3) The method description of ripple-spindle coupling detection is missing.*

We have added the description of ripple-spindle coupling detection in the Methods.

> *(4) Based on Figure 6D, the authors report that ripple-coupled spindles are significantly shorter than isolated spindles. What are the measurements reported on lines 206-207, and how do they relate to the averaged spectrograms shown in Figure 6D?*

Spindle duration was calculated as the time between spindle onset and offset (as described now in the Methods and Figure 7 legend). Ripple-coupled spindle was considered if at least one ripple occurred between the spindle onset and offset. The duration of ripple-coupled and uncoupled spindles was statistically compared (the stats is reported in text). In Figure 7E, the peri-event averaged EEG spectrograms are plotted for isolated and ripple-coupled spindles, highlighting the difference in the event duration.

> *(5) None of the color scales have legends (Figures 2A, B, C, Figure 3D, etc.).*

We have added the color scales on all Figures.

> *(6) Description of what is represented in the box plots is missing.*

We have added the description.

> *(7) Figure 4C, D, legend for the color code is missing.*

We have added color scales legends.

> *(8) Figure 5A legend, assuming this should read intra-ripple frequency instead of inter-ripple.*

We corrected the typo.

> *(9) Figure 5E, while LC units are not modulated before, it could still be informative to overlay the z-scored firing rate on the same graph for comparison.*

Figure 6E (original Figure 5E) shows overlay for awRipples and isoRipples.

> *(10) The discussion states a 4s resolution for cortical state quantification (line 237), but the methods mention 2.5s (line 382).*

We corrected this discrepancy.

> *(11) Results, p.5, line 138, Methods and materials, p.13, line 423: 30% in result text but 20% in method, please correct.*

We corrected this discrepancy.

> *(12) The manuscript cites the biorxiv version of Osorio-Forero et al., but the paper has been published since then; please update.*

We updated this reference.

> *(13) Results, p.2, line 70. The average duration of a session is presented in seconds. Minutes or hours would be more meaningful to the reader.*

We consider this suggestion as optional.

> *(14) Figure 2C is not referenced.*

We added the reference to Figure 2C.

> *(15) Reference missing line 406.*

We added the reference.

> *(16) Lines 352-356: There seems to be an error in the sentence (an extra verb, or an "and" missing somewhere).*

We have corrected this sentence.

> *(17) Figure 3C "synchronization".*

We corrected this typo.

> ***Reviewer #2 (Recommendations for the authors):***
>
> *(1) Line 94 states that "A significant peri-ripple decrease in LC-SUA"; however, which test and how many samples were used are unclear.*

We revised this text as follows: “A significant peri-ripple (± 6 s) decrease in LCSUA, detected by the firing suppression exceeding 2 SDs, was observed in 13 of 15 cases (n = 4 rats).”

> *(2) Line 96 states that "we calculated the modulation onset, duration, and magnitude". Please define modulation before presenting the comparisons.*

We now illustrate the extraction of quantitative variables in Figure 2D.

> *(3) Line 119 states that "we generated surrogate time series for each session by shuffling ripple onset times" which gives the impression that ripple events were shuffled throughout the sleep; however, the method section states that it was jittered within a specific time window for each event. Please clarify the matter.*

We have substantially revised this section to improve clarity and readability.

> *(4) Line 120 states that "Comparisons of SI values before and after ripples and surrogate events confirmed that surrogate events preserved the cortical states in which ripples occurred". Ripple power doesn't seem to be different in pre vs post in the shuffled data (Figure 3B). If ripple timing was randomized, please clarify the observation shown in Figure 3C that the shuffled events had higher SI after than before, as also seen in the real SI data? Please also elaborate what specific groups were significantly different in before vs after bars; data, shuffle, or both?*

We have substantially revised this section to improve clarity and readability.

> *(5) Line 113 and Figure 3A: Because both LC activity and HPC ripples were correlated to SI, the direct relationship between LC and HPC independent of SI (a covariate) was not clear. The authors might be able to conduct a partial correlation analysis to show this effect.*

We appreciate this suggestion and added the correlation plots in Figures 3 and 7. After careful consideration, we believe that the suggested partial correlation analysis does not contribute substantially beyond the main findings already presented.

> *(6) Figure 5A: Inter-ripple frequency needs definition, not provided in the paper nor in the reference paper. The value (180 Hz) suggests a time interval of around 5 ms, which I fail to understand.*

We apologize for this typo. In Figure 6A (original Fig.5A), intra-ripple frequency is plotted. We have corrected this typo in the text and figure legend.

> *(7) Figure 5D: Comparison between aw and sp ripples should also be shown. Please explain the dashed line at 10 (y-axis) a.u.*

Figure 6E (original Fig.5E) shows LC activity around awRipples and isoRipples.

> *(8) Figure 5E: Legend states aw and iso ripples, but the caption says NREM sleep. Please clarify this matter.*

We have revised Figure 6 legend (original Figure 5).

> *(9) Figure 6B: If the spindle time is permuted randomly, why is LC activity in the permuted data still modulated by the spindle times? Can you test the significance of the modulation index of the shuffled data?*

The LC modulation around shuffled time points was not significant. Figure 7C shows LC modulation dynamics around spindles; brown trace showing state-corrected LCMUA trace (after subtraction of LC-MUA around shuffled events).

> *(10) Line 203: Is the unit in Hz (events per second) correctly calculated or shown? ~15 events per second seems arbitrarily large.*

We corrected the units for the event rate. We report the mean oscillatory frequency of spindles ~15 Hz, not events per second.

> *(11) Line 207 states that "neither the LC-MUA rate nor SIs differed during a 2-sec time window preceding either group of spindles"; however, from Figure 6E, the average trace and errors around them (errors need to be stated clearly, for e.g., SEM or SD) show that they are non-overlapping and different. I suspect tests such as the rank-sum test, which test the difference in the central tendencies (as opposed to the KS test, which tests the overall trend in the distribution of the continuous data), might reveal the difference between these values.*

We compared the absolute (not normalized) LC-MUA rate and SI during 2 sec time window preceding spindle onset and did not find any statistical differences. In Figure 7F, the difference during ~ 2 sec before the spindle onset is due to the z-score normalization to their own baseline.

We revised the Result text to improve clarity.

> *(12) Line 209: Modulation seems to be greater in ripp-spindles as shown in fig 6E-F, yet, the text and the interpretation are the opposite i.e,. iso spindles had greater modulation. Hence, authors might have to provide further clarifications or analyses.*

We corrected the labelling in all plots.

> *(13) Line 316: Claims of "suppression of noradrenergic system facilitating the generation of hippocampal ripples and sleep spindles by memory synchrony" are not fully supported by data, as the data seem to be correlational. Also, claims of "preserved LC activity during ripples coinciding with sleep spindles suggest a role for NE in facilitating cross-regional communication underlying memory-related information transfer" lack clarity and contradict the earlier mechanism. Both "suppression" as well as "preservation" of LC neurons are proposed to mechanistically support memory synchrony and/or consolidation in two different brain states (awake and sleep). The authors might need to clarify how both suppression as well as preservation (which I assume is not an activation or positive modulation) of LC neurons can help in memory synchrony or consolidation.*

We revised this part of discussion by making it less speculative.

> ***Reviewer #3 (Recommendations for the authors):***

> *I would recommend that the authors optimize their figure and result presentation, as the current version of the manuscript is unclear in several places, limiting the interpretation of results.*

We substantially revised the manuscript to improve the results presentation and readability.

> *(1) Multiple results are described but not shown quantitatively. Please plot quantifications and statistics (mean {plus minus} error and individual values) in relevant figures. For example, the results referenced on p. 4 (l. 113-116), p. 5 (l. 129-133, 143-147), p. 6 (l. 159161), p. 7 (l. 188-190), and p. 8 (l. 203-207) should be supported by explicit data plots.*

We have revised the manuscript to ensure all results are supported by quantitative and statistical analyses. We revised figures and legends and added new plots showing individual datapoints.

> *(2) Improvements in figures and descriptions are needed. Below are some examples I found:*
>
> *(a) All figures with color scales lack labeling of the color axis, i.e., measure and unit.*

We have revised the figures accordingly.

> *(b) Use precise labeling of axes such as "ripple-band power" and "LC-MUA firing rate", rather than just "power" and "firing rate".*

We have revised the figures accordingly.

> *(c) Figure 1: Indicate behavioral state (wake vs. sleep) in the example trace.*

We have indicated the behavioral state (quiet awake) in the figure legend.

> *(d) Define "peri-ripple" windows explicitly (e.g., {plus minus}6 s or {plus minus}30 s).*

We have revised the text and figure legends accordingly.

> *(e) Clarify how "modulation magnitude" is calculated (line 96).*

We now illustrate the extraction of quantitative variables in Figure 2D

> *(f) Figure 2C: The white overlaid mean trace lacks Y-axis labeling.*

We have added y-axis labeling.

> *(g) Figure 3A: The labeling of "amplitude" is confusing when referring to firing frequency.*

We have corrected the figure labelling.

> *(h) Figure 4B: Is the X-axis time from ripple onset?*

We have corrected the figure labelling.

> *(i) Figure 4C-D lacks an X-axis or color legend.*

We have added x-axis and color legend.

> *(j) Figures 5-6: Include tonic firing rates and time scales.*

We have added in the main text the time scales and average firing rates for LC single units and also show it in Supplementary Figure 1. Because the number of neurons contributing to

LC multi-unit activity (LC-MUA) is unknown, we avoided averaging absolute firing rates for this signal. For LC-MUA, we implemented a normalization approach in which firing rates (50-ms bins) around ripple were scaled to a baseline period preceding the trigger event (−12 to −10 s). Importantly, unlike z-scoring, this normalization method preserved baseline differences across behavioral states, as shown in new Figure 5.

> *(k) Add tonic firing rate baselines where relevant.*

We have added the Supplementary Figure 1 and new Figure 5 showing the difference in the LC baseline firing rate across behavioral states.

> *(3) Minor Comments to add more clarity*
>
> *(a) Clarify "spike train" selection criteria (Methods, p. 4, line 93).*

We revised the text as follows: “In six out of twenty LC-MUA recordings, we could reliably isolate spikes from a total of 15 single units (LC-SUA, n = 4 rats).”

> *(b) Define "EEG transients" (p. 4, line 109) and support with data.*

We revised the text as follows: “Indeed, transient spectral changes in the prefrontal EEG coincided with the occurrence of hippocampal ripples (Figure 2B).”

> *(c) You refer to Figure 3E as a histogram (p. 5, line 128), but I believe it shows an average trace.*

We have corrected this typo.

> *(d) Standard sleep scoring procedures normally involve EMG measurements (p. 6, line 154).*

We have replaced ‘standard’ with “previously established”.

> *(e) Explain how surrogate shuffling preserves the distribution of behavioral states.*

We revised the text as follows: “We first verified that hippocampal LFPs (140– 250 Hz) triggered on these surrogate events lacked the ripple-specific frequency component (Figure 3C), and that the SI state did not differ between real ripples and surrogate events (Figure 3D).”

> *(f) You refer to inter-ripple frequency (p. 6, line 168), which suggests time between ripples. Do you mean the "intra-ripple" or simply ripple frequency?*

We have corrected this typo.

> *(g) Ensure all references cited in the text (e.g., p. 12, line 406) are included in the bibliography.*

We have updated the bibliography.

> *(h) On p. 10, line 304-305 authors refer to observations related to offline memory consolidation. However, the present study does not contain any behavioral memory data.*

We have revised the Discussion to make it less speculative about the role of describe LC dynamics for offline memory consolidation.

References

Novitskaya Y, Sara SJ, Logothetis NK, Eschenko O (2016) Ripple-triggered stimulation of the locus coeruleus during post-learning sleep disrupts ripple/spindle coupling and impairs

memory consolidation. Learn Mem 23:238-248.

Yang M, Logothetis NK, Eschenko O (2019) Occurrence of Hippocampal Ripples is Associated with Activity Suppression in the Mediodorsal Thalamic Nucleus. J Neurosci 39:434-444.

Yang M, Logothetis NK, Eschenko O (2021) Phasic activation of the locus coeruleus attenuates the acoustic startle response by increasing cortical arousal. Sci Rep 11:1409.

https://doi.org/10.7554/eLife.109159.2.sa0